ANL-ARC-251

Report on the Initial Fundamental Sodium-CO_2 Interaction Experiment

Nuclear Engineering Division

About Argonne National Laboratory
Argonne is a U.S. Department of Energy laboratory managed by UChicago Argonne, LLC under contract DE-AC02-06CH11357. The Laboratory's main facility is outside Chicago, at 9700 South Cass Avenue, Argonne, Illinois 60439. For information about Argonne and its pioneering science and technology programs, see www.anl.gov.

DOCUMENT AVAILABILITY

Online Access: U.S. Department of Energy (DOE) reports produced after 1991 and a growing number of pre-1991 documents are available free via DOE's **SciTech Connect** (http://www.osti.gov/scitech/)

Reports not in digital format may be purchased by the public from the National Technical Information Service (NTIS):

U.S. Department of Commerce
National Technical Information Service
5301 Shawnee Rd
Alexandra, VA 22312
www.ntis.gov
Phone: (800) 553-NTIS (6847) or (703) 605-6000
Fax: (703) 605-6900
Email: **orders@ntis.gov**

Reports not in digital format are available to DOE and DOE contractors from the Office of Scientific and Technical Information (OSTI):

U.S. Department of Energy
Office of Scientific and Technical Information
P.O. Box 62
Oak Ridge, TN 37831-0062
www.osti.gov
Phone: (865) 576-8401
Fax: (865) 576-5728
Email: **reports@osti.gov**

Disclaimer
This report was prepared as an account of work sponsored by an agency of the United States Government. Neither the United States Government nor any agency thereof, nor UChicago Argonne, LLC, nor any of their employees or officers, makes any warranty, express or implied, or assumes any legal liability or responsibility for the accuracy, completeness, or usefulness of any information, apparatus, product, or process disclosed, or represents that its use would not infringe privately owned rights. Reference herein to any specific commercial product, process, or service by trade name, trademark, manufacturer, or otherwise, does not necessarily constitute or imply its endorsement, recommendation, or favoring by the United States Government or any agency thereof. The views and opinions of document authors expressed herein do not necessarily state or reflect those of the United States Government or any agency thereof, Argonne National Laboratory, or UChicago Argonne, LLC.

ANL-ARC-251

Report on the Initial Fundamental Sodium-CO_2 Interaction Experiment

Craig Gerardi, Mitchell T. Farmer, Dennis J. Kilsdonk, Robert Aeschlimann, James J. Sienicki, and Christopher Grandy
Nuclear Engineering Division
Argonne National Laboratory

September 28, 2012

ABSTRACT

The U.S. Department of Energy (U.S. DOE) Advanced Reactor Concepts (ARC) Program is developing the Sodium-Cooled Fast Reactor (SFR) as a reactor that could dramatically improve performance in sustainability, safety, economics, security, and proliferation resistance. The near-term Program goal is to reduce technical barriers to improve the prospects of advanced technology reactor systems. In the long-term, integrated advanced reactor system designs will be developed that implement the chosen missions and complete the testing and demonstration necessary for licensing. The supercritical carbon dioxide (S-CO_2) Brayton cycle, coupled with an SFR, has been identified as a new and innovative energy conversion technology that could contribute to meeting these objectives especially in terms of improving economics.

One appealing feature of this energy conversion system is the smaller footprint that the hardware requires relative to the traditional superheated steam cycle, which is in part due to the use of Printed Circuit Heat Exchanger^{TM} (PCHE^{TM}) compact diffusion-bonded heat exchangers as the heat source heat exchanger (sodium-to-CO_2) as well as the recuperator and cooler modules. Although PCHEs have a high degree of structural integrity, the potential for leaks to develop between the sodium and CO_2 coolant channels in the secondary heat exchanger cannot be ruled out, leading to discharge of high pressure CO_2 into the secondary coolant circuit. Due to the robustness of the PCHE design, catastrophic failure leading to CO_2 jet blowdown into the intermediate sodium loop is not deemed likely. Rather, small cracks (or micro-leaks) may develop in which CO_2 will bleed into the secondary system at a relatively low rate and chemically react with the sodium. The 2012 Sodium Fast Reactor Research Plan produced by Sandia National Laboratory (Denman et al., 2012) identified the interaction between sodium and CO_2 as being among the highest priority areas of research for SFR accident initiators. In fact, the report rated both the experimental database and modeling capabilities of Na-CO_2 interactions at the lowest current state of knowledge compared with the other listed high-priority accident initiator items.

In recognition of the anticipated failure mode for a PCHE sodium-to-CO_2 heat exchanger, an Argonne experiment program, called SNAKE, was initiated in FY 2010 to investigate the reaction characteristics between sodium and CO_2 under micro-leak conditions. The goal of the SNAKE facility is to:

1. Determine the fundamental nature and extent of the chemical reactions that occur between high-pressure CO_2 issuing into liquid sodium from a micro-leak across a stainless steel pressure boundary as a function of the sodium pool temperature and inlet CO_2 flowrate,
2. Examine the potential for the micro-leak to seal itself up as a result of blockage formation from the chemical reaction byproducts of the Na-CO_2 reaction, or as a result of oxide layer buildup on the crack faces,
3. Develop one-dimensional phenomenological models for the interactions between high-pressure CO_2 issuing into liquid sodium from a micro-leak across a stainless steel pressure boundary. These models will be validated using the experiment data obtained during the completion of the previous two objectives.

This report provides an update on the facility status and the first sodium-CO_2 experiment. This test was successful in that supercritical carbon dioxide was sparged into a pool of sodium through a 64 µm diameter nozzle. Approximately 125 standard liters of CO_2 were injected into a 38.1 cm (15 inch) high column of sodium at 170 ˚C over the course of 30 minutes at a pressure of approximately 9.0 MPa (1300 psi). This is the first known test involving supercritical CO_2 and sodium. Preliminary data analysis suggests that a small amount of carbon monoxide was produced from the reaction between sodium and CO_2. No plugging of the micro-nozzle was detected during this experiment. Further analysis is required prior to unequivocally stating that CO was produced in this test. More detailed analysis of this set of data and planning for improving data quality and facility control will take place in early FY 2013.

Fiscal Year 2013 will include formulating an experiment test matrix and making additional hardware improvements to improve data quality, with a detailed report delivered in September 2013. A number of lessons were learned from the first shakedown experiment, which has led to suggested facility improvements. These improvements will also take place in FY 2013. Model development and validation will take place the following Fiscal Year, with a detailed model report anticipated to be delivered in September 2014.

Table of Contents

Abstract i

List of Figures iv

List of Tables vi

1 Introduction 1

Background 1
International work on sodium-CO_2 interactions 4
Approach 5

2 Facility Design Description 6

Facility design 11

3 FY 2012 Status 15

Data acquisition interface designed and programmed 16
Sodium loading 21
Miscellaneous activities 22

4 Shakedown Tests and Data 29

Gas system blowdown into water 29
Test vessel filling with sodium checkout 31
First fundamental sodium-CO_2 interaction experiment 33

5 Lessons Learned from the First Test and Future Work 39

6 Summary 42

References 44

LIST OF FIGURES

Figure 1: Schematic illustration of a S-CO_2 Brayton cycle power conversion system coupled to a pool-type SFR. 1
Figure 2: Schematic of potential microcrack formation mechanism in a PCHE and subsequent sodium-CO_2 reaction. 3
Figure 3: Updated schematic showing key components of the sodium-CO_2 reaction test facility. 8
Figure 4: Updated drawing of sodium components of the sodium-CO_2 reaction test facility. 9
Figure 5: Recent picture of fully-assembled SNAKE facility. 10
Figure 6: (left) Drawing of CO_2 micro-nozzle connected to high-pressure gas delivery line in a cutaway of the test vessel and (right) picture of one of the fabricated nozzles. 12
Figure 7: Test vessel with a researcher below for scale. 13
Figure 8: CO_2 Pre-heater installed near test section 14
Figure 9: (left) Picture of dump tank wrapped in a layer of flexible alumina insulation and (right) picture of stainless box with dump tank inside. 14
Figure 10: Facility with data acquisition PC shown. 16
Figure 11: Screenshot of DAS system showing facility temperature schematic during an experiment run. 17
Figure 12: Mass spectrometer mounted on outside of SNAKE facility. The duct that runs to the scrubber is pictured at the top, while two wire terminal boxes that contain the heater controller wires are located above the mass spectrometer. 23
Figure 13: Heater tape wrapped around the tubing and valves that run between the test section (top right) and dump tank (not pictured – bottom left). The emergency dump valve is located in the center of the photograph. 24
Figure 14: Control rack with National Instruments chassis on top, valve control panel in the middle, and instrument power near the bottom. 25
Figure 15: Nozzle and gas line installed on test vessel. 26
Figure 16: Permanent installation of vacuum pump to facilitate pump-down of either test vessel or dump tank. 27
Figure 17: Assembled state of the SNAKE facility as of September 2012 (4 front doors are open to view interior). 28
Figure 18: Glass tank with micro-nozzle assembly installed. This tank can be filled with water which allows for visualization of the blowdown of S-CO_2 into a fluid. 29
Figure 19: Supercritical CO_2 at 7.8 MPa sparging into water from a micro-nozzle assembly. 30
Figure 20: Temperatures of select dump tank and test vessel rake thermocouples during sodium filling of the test vessel. 32

Figure 21: Measured CO_2 flow rate through the Coriolis flow meter in g/hr (top). Measured gas density (left) and conversion to standard liters per minute (right). A moving average was used to clean up the curve and remove noise. 33
Figure 22: Pressures of the test vessel and CO_2 reservoir.....34
Figure 23: Nozzle temperature during first sodium-CO_2 test 35
Figure 24: Thermcouple rake temperatures during first sodium-CO_2 test. A moving average was used to clean up the curve and remove noise. 36
Figure 25: Raw mass spectrometer data comparing the relative peak heights of argon, carbon dioxide and carbon monoxide for two tests. Solid lines represent a test where carbon dioxide was vented through the micro-nozzle into the empty heated test vessel. Dotted lines represent a test where carbon dioxide was vented through the micro-nozzle into the test vessel under comparable conditions with the addition of sodium being present in the vessel. 37
Figure 26: Fraction of Mass 44 (CO_2) divided by Mass 28 (CO) detected. A moving average was used to clean up the curve and remove noise. 38

LIST OF TABLES

Table 1: SNAKE Facility Specifications 6
Table 2: SNAKE DAS Channel Hookup 18
Table 3: Standard Cracking Patterns for CO_2 and CO. Highest Peak Normalized to 100 37

1 Introduction

Background

The U.S. Department of Energy (U.S. DOE) Advanced Reactor Concepts (ARC) Program is developing the Sodium-Cooled Fast Reactor (SFR) as a reactor that could dramatically improve performance in sustainability, safety, economics, security, and proliferation resistance. The near-term Program goal is to reduce technical barriers to improve the prospects of advanced technology reactor systems. In the long-term, integrated advanced reactor system designs will be developed that implement the chosen missions and complete the testing and demonstration necessary for licensing. The supercritical carbon dioxide (S-CO_2) Brayton cycle, coupled with an SFR, has been identified as a new and innovative energy conversion technology that could contribute to meeting these objectives especially in improving economics. This system, depicted schematically in Figure 1, removes energy from the intermediate sodium circuit in a pool-type reactor plant or the primary or intermediate sodium circuit in a loop-type plant and converts it into electrical energy at greatly improved thermal efficiencies over comparable Rankine cycle conversion schemes depending upon the reactor core outlet sodium temperature. The S-CO_2 Brayton cycle was identified as the primary energy conversion system of interest under the ARC Program and evaluation of the chemical reactions between the reactor coolant and balance of plant fluid was specifically mentioned as a program goal (ARC, 2011).

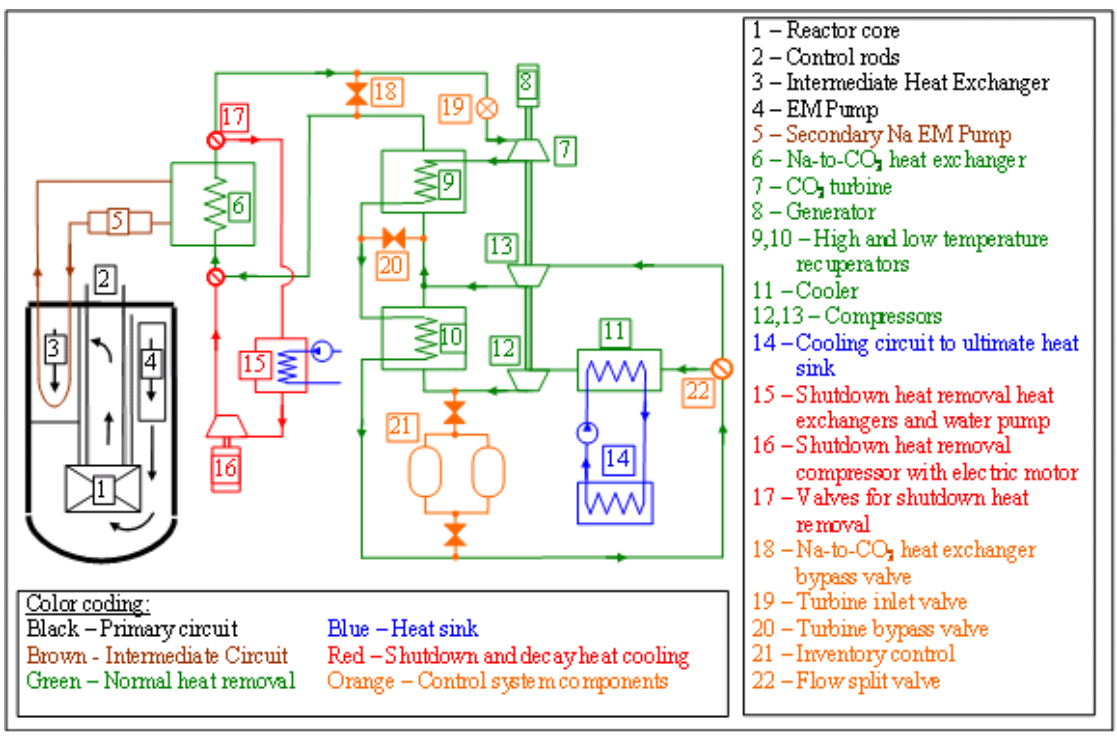

Figure 1: Schematic illustration of a S-CO_2 Brayton cycle power conversion system coupled to a pool-type SFR.

A major benefit of the S-CO_2 Brayton cycle is elimination of the potential for energetic sodium-water reactions which result in the formation of combustible hydrogen gas. Desirable attributes for this system include: 1) reduction in power conversion system costs relative to the Rankine steam cycle by taking advantage of the small sizes of the turbine and compressors as well as the fewer number of components [i.e., the condenser, feedwater heaters, and deaerator of the Rankine cycle are eliminated]; and 2) higher thermal efficiency relative to the Rankine steam cycle especially at the higher reactor core outlet temperatures of some sodium-cooled fast reactor concepts.

Operating pressures are 20 MPa or higher at the compressor outlets and remain above the CO_2 critical pressure of 7.377 MPa at the compressor inlets during normal operation and nominal load. The CO_2 temperature remains above the CO_2 critical temperature of 30.98 °C during normal operation. The components including the turbine and compressors must be manufactured from alloys that are resistant to corrosive oxidation attack by CO_2 while also meeting other structural requirements. It is well know that austenitic stainless steel has exhibited outstanding corrosion resistance to CO_2 attack at prototypical pressures and temperatures in S-CO_2 corrosion loop tests and is a material of choice for S-CO_2 Brayton cycle components and piping.

One feature contributing to footprint reduction for this system is the use of Printed Circuit Heat Exchangers (PCHEs) (Li et al., 2006) as the heat source heat exchanger (Na-to-CO_2) as well as the recuperator and cooler modules. PCHEs are high integrity plate type heat exchangers that are fabricated from flat metal plates that have fluid flow channels formed via chemical etching using a process similar to that developed for electronic printed circuit board production. The etched plates are stacked and diffusion bonded together to make the core of the heat exchanger. These units can be four to six times smaller than conventional shell-and-tube heat exchangers of the equivalent heat duty, and they can have pressure and temperature capabilities in excess of 600 bar and 900°C, respectively.

Although PCHEs have a high degree of structural integrity, the potential for leaks to develop between the sodium and CO_2 coolant channels in the secondary heat exchanger cannot be ruled out, leading to discharge of high pressure CO_2 into the secondary coolant circuit. Due to the robustness of the PCHE design, catastrophic failure leading to CO_2 jet blowdown into the secondary sodium loop is not deemed to be a likely scenario. Heatric claims that the pressure-boundary failure mechanism observed when gas-to-gas PCHEs have failed due to customer misuse consists only of slow leakage due to the formation of small cracks between the streams (Chang et al., 2006). It is thus expected that small cracks (or micro-leaks) may develop in which CO_2 will bleed into the sodium at a relatively low rate and chemically react with the sodium (see Figure 2 for a schematic of this interaction). The former (CO_2 jet) scenario is more relevant for shell-and-tube heat exchanger designs that do not have the monolithic construction features characteristic of PCHEs. Modeling and experiments addressing this case have been carried out by Gicquel et al. (2010) and Gerardi et al. (2010). The primary focus of the current work is to develop an experiment capability to investigate reaction characteristics under micro-leak conditions. Some research (Eoh et al., 2010) on microcrack leaks of CO_2 into sodium has been carried out by the Korea Atomic Energy Research Institute (KAERI) subsequent to the initiation of the current project. Some important distinctions between the KAERI work and the current project include the CO_2 injection pressure (the KAERI work had a maximum CO_2 pressure of 55 bar, vs. 200 bar for

the current project), sodium pool height (~0.4 m for the KAERI work, vs. ~1.0 m for the current project), and the crack size investigated (the KAERI work evaluated sizes greater than 300 microns, while the present work will examine sizes as low as 50 microns).

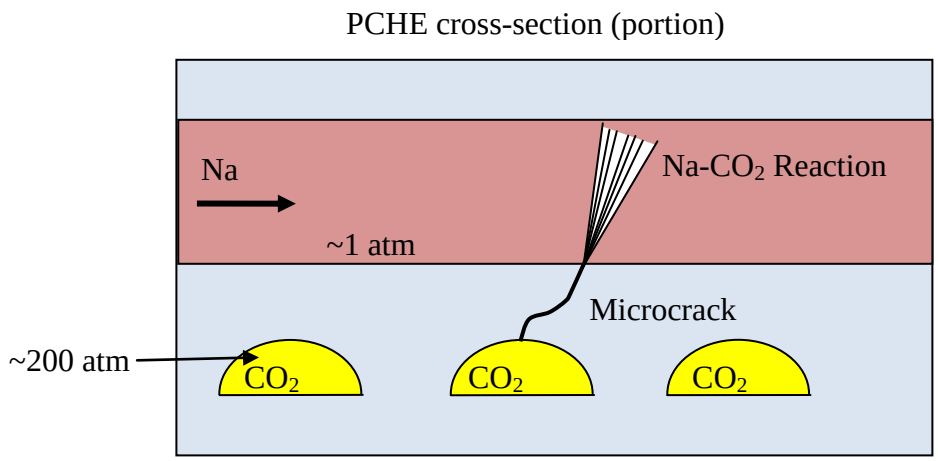

Figure 2: Schematic of potential microcrack formation mechanism in a PCHE and subsequent sodium-CO_2 reaction.

As discussed by Gicquel et al. (2010), two Na-CO_2 chemical reaction scenarios are possible. In particular, for a temperature below ~ 500 ºC, the CO_2 reacts with sodium, principally forming sodium oxalate ($Na_2C_2O_4$) and carbon monoxide (CO). The oxalate then further reacts with the sodium to form oxide (Na_2O). The reactions are of the form (Gicquel et al., 2010),

$$Na + CO_2 \rightarrow \frac{1}{4} Na_2C_2O_4 + \frac{1}{4} CO + \frac{1}{4} Na_2CO_3$$
$$4Na + Na_2C_2O_4 \rightarrow 3Na_2O + CO + C \qquad (1)$$

The carbonate is effectively inert in the sodium, remaining as a solid solution that can precipitate out within the system with potentially undesirable consequences. Oxygen is normally present in the coolant at ppm levels; the oxide may decompose or remain in solution depending upon the oxygen potential in the coolant. The CO can react with sodium also, but the kinetics of this reaction are much slower than the sodium-oxalate reaction (Gicquel et al., 2010) and so the potential exists for the monoxide to loiter in the solution for some (undetermined) length of time, possibly passing out of the system as a gas that could accumulate at high points in the secondary sodium loop.

As noted earlier, above ~ 500 ºC the Na-CO_2 reaction takes a different form. In particular, the sodium rapidly reacts with the gas to form elemental carbon as well as carbonate; i.e. (Gicquel et al., 2010),

$$Na + \frac{3}{4}CO_2 \rightarrow \frac{1}{4}C + \frac{1}{2}Na_2CO_3 \quad (2)$$

As is evident from this equation, in this temperature regime there is no gaseous byproduct from the reaction. Moreover, the carbonate remains as an inert solid in solution with the sodium.

The above discussion indicates that if a small leak in a compact heat exchanger were to develop, then solid byproducts (principally sodium carbonate) will be formed below ~ 500 ºC. One question that arises is whether or not the carbonate that forms could possibly plug the leak over time, yielding the beneficial outcome that the small leaks are self-healing. Potential also exists for oxide buildup on such a small crack due to the high temperature CO_2 passing over stainless steel, and for enlargement of small cracks due to high thermal stresses near the nozzle due the Na-CO_2 reaction. These are some of the principal questions to be addressed as part of this work, along with evaluating the chemical reaction characteristics under low flow conditions.

International work on sodium-CO_2 interactions

As mentioned above, several other research organizations are in the process of developing experiment and modeling capabilities to understand the sodium-CO_2 reaction. The primary organizations studying this reaction are the Korea Atomic Energy Research Institute (KAERI) and the Commissariat à l'énergie atomique et aux énergies alternatives (CEA). The CEA work (Gicquel et al., 2010; Gicquel et al., 2011) primarily is focused on larger breaks typical of a shell-and-tube type rupture (jetting), and has been carried out at subcritical pressures. No plans to study the effect of CO_2 pressure on the reaction are known. They are currently developing an analytical model for CO_2 jetting into a pool of sodium, which includes a reaction model. At this time, their model does not do a good job of predicting the experiment results. They do report a threshold temperature of approximately 500 ˚C, above which the reaction becomes extremely energetic. Their jetting experiments include a mass spectrometer to evaluate carbon monoxide production, and some calorimetric work was completed to evaluate the reaction enthalpies. Their modeling work consists of modifying and improving existing steam jetting into sodium models. They are extensively evaluating the velocities and temperatures throughout the jet, which is the validation objective of their experiments. The model is complicated by the three-phase nature of the reaction and the complicated kinetics of the primary reactions.

The KAERI work (Eoh et al., 2010) is examining two issues: 1) wastage of stainless steel in a sodium pool due to impact by a CO_2 jet, and 2) understanding the reaction between sodium and CO_2. The first issue is important for both shell-and-tube heat exchangers and PCHEs in that a single failure could cascade into multiple tube (or channel) ruptures should the wastage effect be strong. However, this issue is beyond the scope of the present work. The second issue that KAERI is studying is very much related to the present work. They have done simple surface reaction tests by blowing CO_2 across the surface of a small sodium pool over a large range of temperatures (200 ˚C – 600 ˚C). They used a mass spectrometer to analyze the reaction gases and several diagnostic approaches to examine the solid reaction products after each test. While these tests are not prototypic of PCHEs, they add much to the knowledge base regarding the reaction itself, including kinetic parameters. They also have an

experiment program investigating more PCHE prototypic geometries and conditions. They have injected gas bottle pressure (5.5 MPa) CO_2 at several temperatures (400 ˚C & 550 ˚C) through small holes (down to 0.3 mm) into a small diameter (2 mm) sodium channel. These channels did not plug after several minutes of CO_2 injection. Lastly, they have injected low pressure (0.5 MPa) CO_2 through larger cracks (0.5-1.5 mm) into sodium pools at a range of temperatures (300 ˚C – 600 ˚C). Some plugging of the smaller nozzles (<1.5 mm) as seen for low initial leak rates at high temperatures (> 500 ˚C).

There is a clear niche for obtaining data for truly prototypic heat source heat exchanger conditions namely at high pressure (20.0 MPa) and for small crack sizes (< 100 µm), which the present project will attempt to provide.

Approach

The purpose of this work is to develop the capability to conduct well-controlled experiments that can achieve the following two technical objectives:

1. Determine the fundamental nature and extent of the chemical reactions that occur between high-pressure CO_2 issuing into liquid sodium from a micro-leak across a stainless steel pressure boundary as a function of the sodium pool temperature and inlet CO_2 flowrate,
2. Examine the potential for the micro-leak to seal itself up as a result of blockage formation from the chemical reaction byproducts of the sodium-CO_2 reaction, or as a result of oxide layer buildup on the crack faces,
3. Develop one-dimensional phenomenological models for the interactions between high-pressure CO_2 issuing into liquid sodium from a micro-leak across a stainless steel pressure boundary. These models will be validated using the experiment data obtained during the completion of the previous two objectives.

The experiment approach for achieving these objectives is to construct a well-instrumented test facility that consists of a vessel containing molten sodium with a test specimen that mocks up a micro-crack in a PCHE located at the bottom of the pool. High-pressure CO_2 is bled through the crack under controlled (i.e., constant pressure and temperature) conditions; flowrate through the crack is monitored over time to determine if the crack plugs and, if so, the rate at which plugging occurs. The gas composition is monitored with a gas mass spectrometer to determine the gaseous byproducts that are expected to evolve from the chemical reactions described above; local sodium temperatures around the crack are also monitored. Post-test examination of solid reaction products will also be possible. Aside from examining the potential for a micro-crack to plug, these data provide additional information to validate the proposed chemical reaction sequences given by Gicquel et al. (2010) that were outlined above.

The balance of this report describes progress made towards meeting these objectives so far this fiscal year. An experiment facility called SNAKE (S-CO_2, Na Kinetics Experiment) has been designed and assembled in the Building 206 High-Bay at Argonne National Laboratory. A summary of the underlying scaling rationale and facility design was provided in (Gerardi et al., 2011). A report describing the completion of SNAKE assembly and loading of sodium during was provided in (Gerardi et al., 2012). This report describes the first sodium-CO_2

interaction experiments. Planning for the modeling approach to complete Objective 3 will be prepared in FY 2013, while actual modeling and validation work will begin in FY 2014. No further discussion of modeling plans will be made in the present report.

2 Facility Design Description

An initial design description was provided in 2010 (Farmer et al., 2010) for a facility focused on investigating sodium-CO_2 reactions under conditions that mock up a small leak within a PCHE. That document provided the starting point for further design improvements, detailed specifications, and purchases in FY 2011. Changes and improvements to the original facility design were made in FY 2011 (Gerardi et al., 2011) and through June 2012 (Gerardi et al., 2012). This report summarizes the current facility design and discusses the first shakedown experiments completed in September 2012.

A schematic and three-dimensional rendering of the SNAKE facility are provided in Figure 3 and Figure 4, respectively. Key features and specifications for the facility are summarized in Table 1. A recent picture of the facility fully assembled is shown in Figure 5.

Table 1: SNAKE Facility Specifications

Parameter	Value
General	Sodium-CO_2 chemical reaction experiment
Overall facility height	3.65 m (12 ft)
Maximum temperature and pressure rating of sodium vessels	3.1 MPa (450 psi) at 510 ˚C
Maximum CO_2 gas pressure	20.6 MPa (3000 psi)
CO_2 nozzle diameter range	60-100 µm
Maximum sodium column pool height as currently configured	0.80 m (2.6 ft)
Maximum CO_2 volumetric flowrate	5.8 slpm
Sodium column diameter	10 cm (4 inches)
Key Instruments	1) CO_2 flowmeter with 0.5-2.4% measurement uncertainty 2) Mass spectrometer for analyzing exhaust gasses 3) Wireless pressure transmitters for line pressures 4) Laser level indicator for sodium level in test vessel 3) Thermocouples at nozzle tip, near nozzle outlet in sodium, and throughout system
Approximate total facility sodium mass	22 kg (40 lb); approximately 21 L (5.5 gallons);
Approximate test vessel sodium volume	9.5 L (2.5 gallons); approximately 8.5 kg (19 lb)
Approximate total heater input power	~ 15 kW

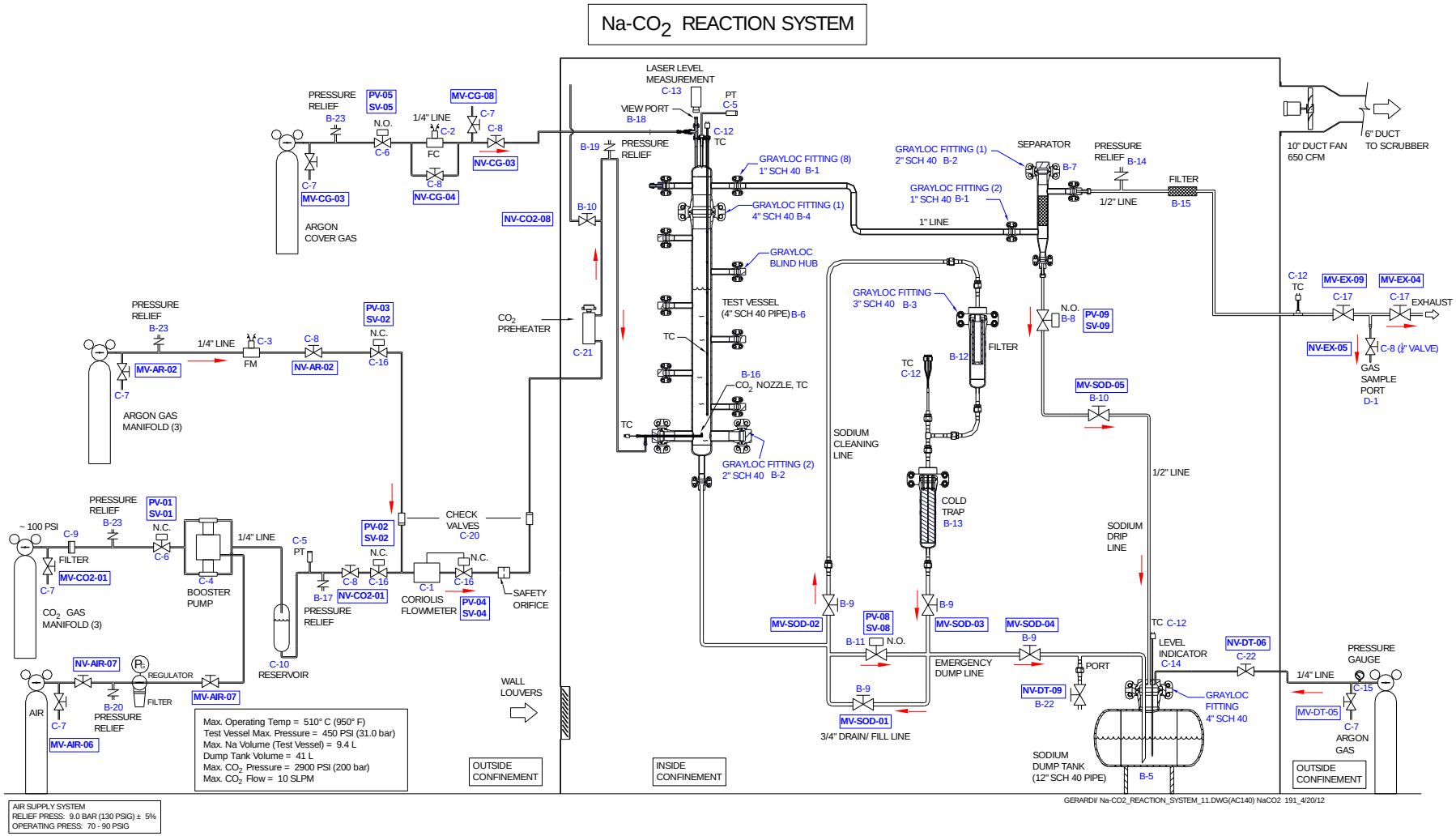

Figure 3: Updated schematic showing key components of the sodium-CO_2 reaction test facility.

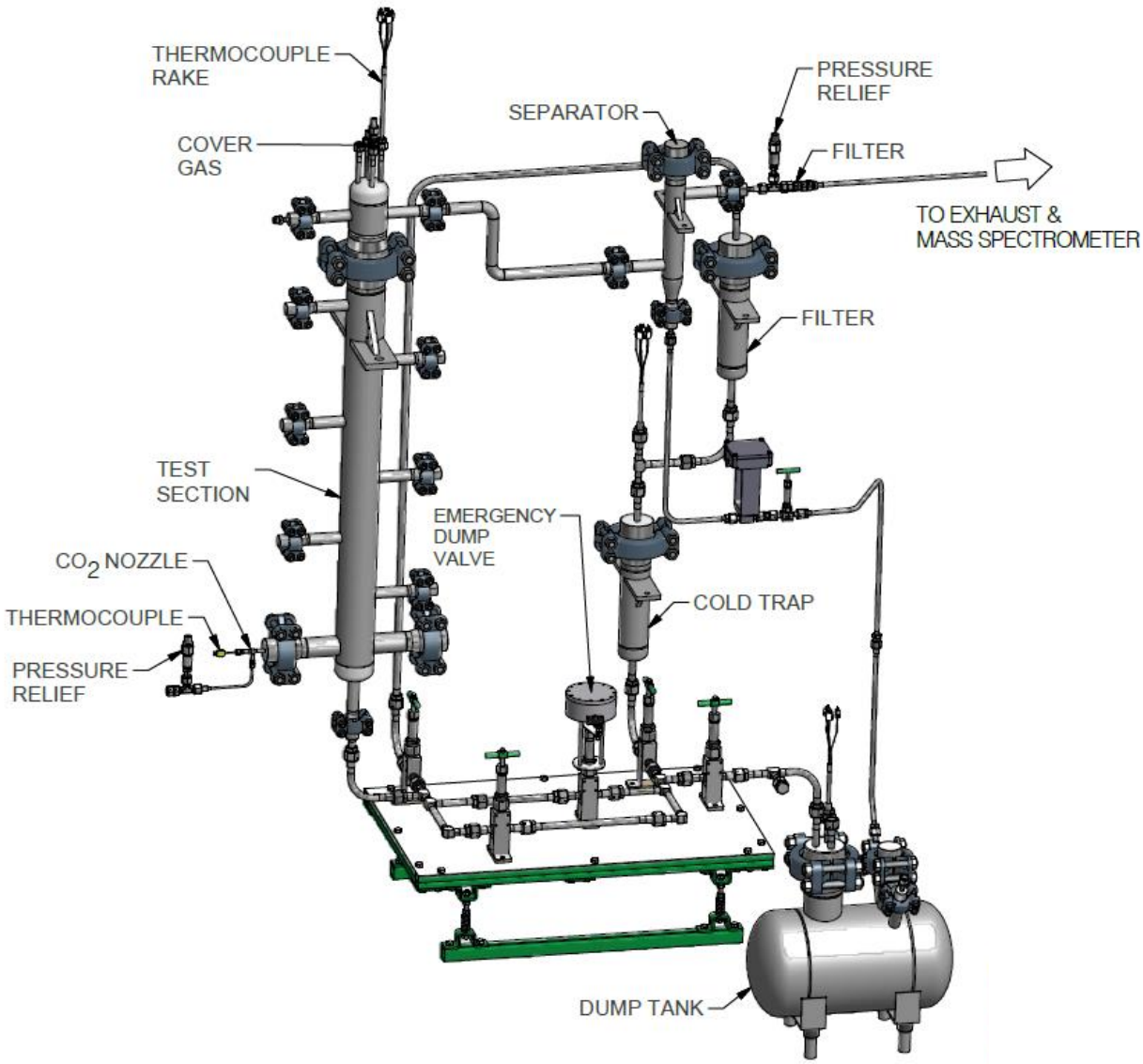

Figure 4: Updated drawing of sodium components of the sodium-CO_2 reaction test facility.

Figure 5: Recent picture of fully-assembled SNAKE facility.

Facility design

As shown in Figure 4 (schematic in Figure 3), the key elements of the test facility consist of the:

i. test vessel,
ii. argon cover gas supply,
iii. CO_2 supply system to the test nozzle that simulates a leak site in a PCHE,
iv. argon supply system to the test nozzle to prevent sodium plugging prior to CO_2 flow initiation,
v. sodium dump system including a filter/cold trap to clean sodium and capture solid reaction products,
vi. off gas system,
vii. confinement system to direct smoke from any accidental sodium spill to the building scrubbing unit,
viii. instrumentation (flow meters, pressure transmitters, level measurement, thermocouples, mass spectrometer, etc.)

One of the key changes made during FY 2012 to the design of the SNAKE experiment was to re-configure the CO_2 injection nozzle. The geometry of the old design (coiled tube inside of the 2" pipe penetration at the bottom of the test vessel) was deemed likely to make nozzle removal and replacement difficult once exposed to sodium. This is because sodium can easily remain in gaps of less than ½ inch between components even after being drained. Once this bridging sodium freezes, it can be difficult to pull components away from each other. This would be problematic especially for the injection nozzle component since it will be replaced between each test. Sodium systems are not typically opened while the sodium is molten.

The new CO_2 injection micro-nozzle (see Figure 6) consists of a 3.2 mm (1/8 inch) seamless 316 stainless steel tube with a machined stainless steel injector tip connected with a welded coupling. The end of each injector tip has a laser machined 63-75 µm diameter hole to form the actual nozzle which will simulate the PCHE microcrack. The tube is welded onto a 5.1 cm (2 inch) Grayloc® blind hub (attached to the bottom horizontal test vessel penetrations) as the nozzle sodium barrier. This new nozzle geometry makes EDM welding of the nozzle components possible, which is a far more robust method of joining them than the method previously considered: Nichrome brazing. Several of these nozzles have been fully fabricated. Approximately 15 additional nozzle tips have been laser drilled with diameters ranging from 60-75 µm. These tips will be welded to the nozzle assembly in FY 2013 for further sodium-CO_2 tests.

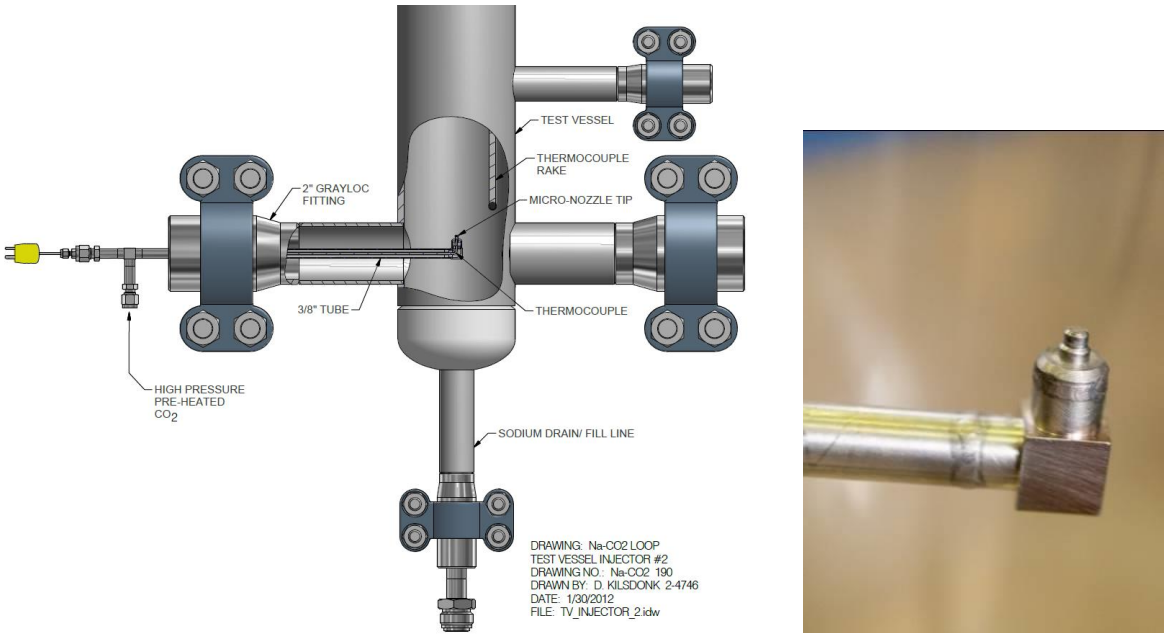

Figure 6: (left) Drawing of CO_2 micro-nozzle connected to high-pressure gas delivery line in a cutaway of the test vessel and (right) picture of one of the fabricated nozzles.

The CO_2 source consists of a traditional bottle manifold that feeds a booster pump. The pump pressurizes a reservoir cylinder that is used to supply a regulated pressure to the leak site of up to 20 MPa (2900 psig) pressure; the reservoir is used to dampen pressure fluctuations that are inherent when the pump is operational. Flow rate to the tube is measured with a Coriolis flowmeter. The occurrence of plugging will be evidenced by the flow rate tending towards zero. The output from the Coriolis flowmeter provides a feedback signal that automatically closes an isolation valve on the feed line to the leak site if the flow rate exceeds a user-defined threshold value. A flow-limiting orifice is positioned downstream of the flowmeter. This is a backup safety device that limits the peak CO_2 flow rate to the test section to an acceptable rate in the unlikely event that the tube feeding the leak and the isolation valve failed simultaneously. This orifice does not result in a significant pressure drop under normal operating conditions.

A photograph of the test vessel with a researcher below it for scale is included in Figure 7.

Figure 7: Test vessel with a researcher below for scale.

A cast aluminum circulation pre-heater (see Figure 8) is capable of heating the CO_2 up to 510 ºC prior to entering the test section. This system has a dedicated over-temperature

protection system. This circulation pre-heater is also a new component purchased in FY 2012. It should give the experimenter much greater control of the inlet CO_2 temperature.

Figure 8: CO_2 Pre-heater installed near test section

A stainless steel box to enclose the sodium dump tank was fabricated. This is a newly designed component to allow for ease-of-insulation of the irregularly-shaped dump tank. The dump tank was first wrapped with a layer of flexible alumina insulation. Then granular vermiculite insulation can be poured into the stainless steel box. This combination will provide ample insulation for the dump tank and make heating time shorter. The vermiculite can then be sucked from the box with a vacuum equipped with a HEPA filter to access the dump tank.

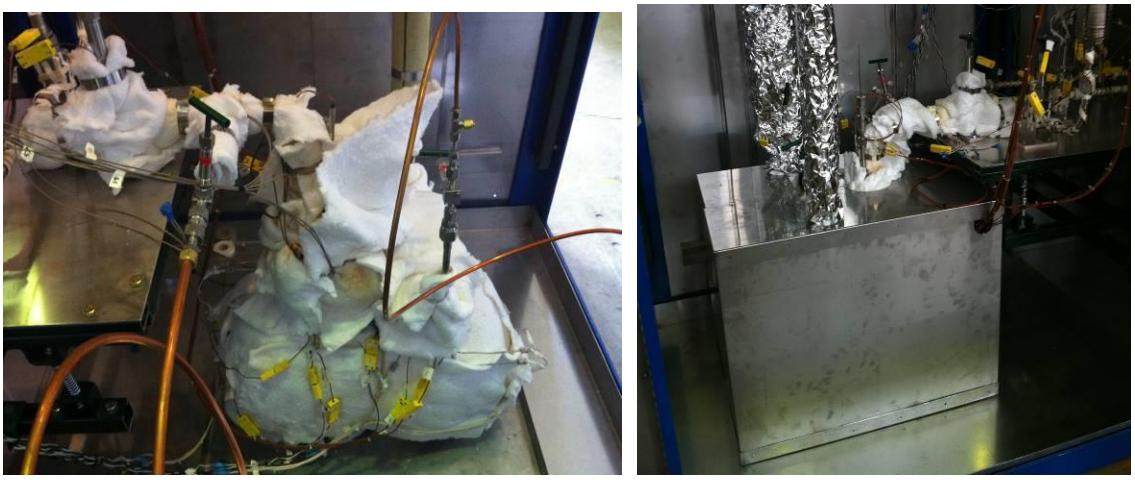

Figure 9: (left) Picture of dump tank wrapped in a layer of flexible alumina insulation and (right) picture of stainless box with dump tank inside.

3 FY 2012 Status

The first sodium-CO_2 interaction experiment was carried out in September 2012. Assembly of the SNAKE experiment was completed in July 2012. The facility design was completed in September 2010 which was detailed in a design report (Farmer et al., 2010). Most major components were purchased, and portions of the facility were assembled in 2011, which was documented in Gerardi et al. (2011). Completion of major component procurement is complete. Minor materials and services (M&S) purchases are ongoing. Fiscal Year 2013 will consist of obtaining substantial data on the interactions between sodium and CO_2, with a sodium-CO2 interaction test matrix delivered in April 2012 and a detailed report delivered in September 2013. Additional improvements and experiments are expected to take place in FY 2013. Model development and validation is planned for the following Fiscal Year, with a detailed model report anticipated to be delivered in FY 2014.

Data acquisition interface designed and programmed

A data acquisition system (DAS) was developed to display and record the SNAKE experiment status and data. This DAS was programmed in LabView 2011 and run on a large display unit next to SNAKE as shown in Figure 10.

Figure 10: Facility with data acquisition PC shown.

The DAS utilizes the producer-consumer (data) design pattern to ensure that all data generated is recorded and displayed without encountering race conditions. A schematic of the facility that includes real-time local vessel and tube temperatures along with thermocouple rake data was designed. This allowed for the capability of determining the status of the facility at a glance. This is, of course, an important feature when moving sodium around the facility and for guaranteeing safe emergency dumping capabilities. A screenshot of the temperature schematic in operation during an experiment is shown in Figure 11. The DAS also records and displays gas flow rates, pressures, level indicators, and mass spectrometer data. A detailed list of the DAS channel numbers associated with each instrument recorded is listed in Table 2.

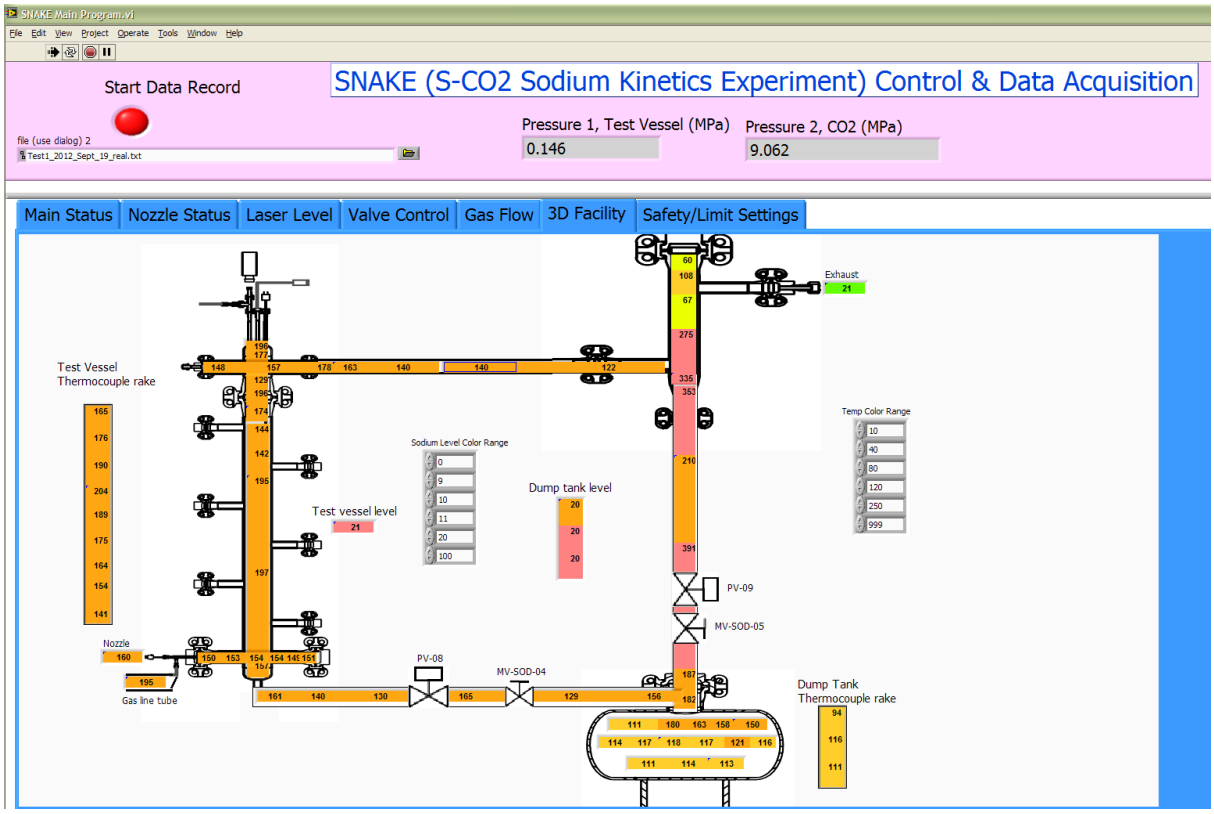

Figure 11: Screenshot of DAS system showing facility temperature schematic during an experiment run.

Table 2: SNAKE DAS Channel Hookup

Labview Channel #	DAS CARD #	DAS Channel #	Thermocouple #	Component located on	Detailed location
0	1	0	41	Test Vessel	2" penetration, north mid
1	1	1	33	Test Vessel	2" penetration, north near body
2	1	2	35	Test Vessel	2" penetration, south CO_2 nozzle near body
3	1	3	36	Test Vessel	2" penetration, south CO_2 nozzle near hub
4	1	4	25	Test Vessel	Body near 2" penetration, east
5	1	5	40	Test Vessel	Body bottom cap
6	1	6	26	Test Vessel	Body near 2" penetration, west
7	1	7	34	Test Vessel	2" penetration, north near hub
8	1	8	32	Test Vessel	1" penetration, bottom-most
9	1	9	31	Test Vessel	1" penetration, 2nd from bottom
10	1	10	24	Test Vessel	Body, middle west
11	1	11	23	Test Vessel	Body, middle east
12	1	12	30	Test Vessel	1" penetration, 3rd from bottom
13	1	13	21	Test Vessel	Body top, south
14	1	14	27	Test Vessel	1" penetration, 6th from bottom
15	1	15	22	Test Vessel	Body top, north
16	1	16	67	Vessel head	Head middle, east
17	1	17	75	1" Line	Middle
18	1	18	66	Vessel head	1" penetration, north near body
19	1	19	28	Test Vessel	1" penetration, 5th from bottom
20	1	20	69	Vessel head	1" penetration, north near 1" line
21	1	21	63	Vessel head	1" penetration, south near hub
22	1	22	70	Vessel head	Head, top of cap
23	1	23	64	Vessel head	Top penetration, west
24	1	24	71	Vessel head	Top penetration, north
25	1	25	65	Vessel head	Top penetration, east
26	1	26	72	Vessel head	Top penetration, center
27	1	27	51	Separator	Body, top
28	1	28	53	Separator	Top penetration
29	1	29	54	Separator	Body, bottom
30	1	30	80	Cold trap	Body, bottom
31	1	31	82	Filter	Body, bottom

32	2	0	7	Dump tank	Body, middle west
33	2	1	3	Dump tank	Body, middle east
34	2	2	5	Dump tank	Body, middle north cap
35	2	3	19	Dump tank	Small penetration, east
36	2	4	9	Dump tank	Bottom, north cap
37	2	5	8	Dump tank	Body, middle east
38	2	6	18	Dump tank	2" penetration, north
39	2	7	10	Dump tank	Body, bottom south
40	2	8	20	Dump tank	4" penetration, east
41	2	9	6	Dump tank	Body, middle west
42	2	10	1	Dump tank	Body, middle south cap
43	2	11	16	Dump tank	Body, bottom middle
44	2	12	14	Dump tank	1" penetration, west drain
45	2	13	13	Dump tank	2" penetration, south
46	2	14	12	Dump tank	1" penetration, east
47	2	15	Empty	Empty	
48	2	16	Empty	Empty	
49	2	17	Empty	Empty	
50	3	0	100	Test section rake	4 cm above nozzle
51	3	1	101	Test section rake	17 cm above nozzle
52	3	2	102	Test section rake	30 cm above nozzle
53	3	3	103	Test section rake	43 cm above nozzle
54	3	4	104	Test section rake	56 cm above nozzle
55	3	5	105	Test section rake	69 cm above nozzle
56	3	6	106	Test section rake	82 cm above nozzle
57	3	7	107	Test section rake	95 cm above nozzle
58	3	8	108	Test section rake	108 cm above nozzle
59	3	9	109	Test section rake	121 cm above nozzle
60	3	10	110	Cold trap rake	Top - 1
61	3	11	111	Cold trap rake	Middle - 2
62	3	12	112	Cold trap rake	Middle - 3
63	3	13	113	Cold trap rake	Middle - 4
64	3	14	114	Cold trap rake	Bottom -5
65	3	15	115	Dump tank rake	Top
66	3	16	116	Dump tank rake	Middle
67	3	17	117	Dump tank rake	Bottom
68	3	18	118	CO_2 Pre-heater exit	
69	3	19	119	CO_2 Pre-heater trip	
70	3	20	120	Enclosure ambient	Bottom
71	3	21	121	Exhaust line	Outside enclosure

72	3	22	122	Enclosure ambient	Top
73	3	23	88	MV-SOD-02	n/a
74	3	24	90	Emergency dump line	n/a
75	3	25	93	Emergency dump line	After PV-08
76	3	26	94	Emergency dump line	Tee out (lower)
77	3	27	95	MV-SOD-03	n/a
78	3	28	96	Manual drain line	near dump tank
79	3	29	97	MV-SOD-04	n/a
80	3	30	98	Manual drain line	middle
81	3	31	50	3/4" Na cleaning line	top
82	4	0	77	1" line	near test vessel
83	4	1	76	1" line	near separator
84	4	2	56	Separator	2" hub
85	4	3	57	Separator	1" top horizontal hub
86	4	4	59	Separator	1" lower vertical hub
87	4	5	60	Exhaust line	Inside enclosure
88	4	6	84	Filter	3" hub
89	4	7	85	Cold trap	3" hub top
90	4	8	86	Cold trap	3" hub bottom
91	4	9	87	Tube below cold trap	n/a
92	4	10	99	Drain line	Above dump tank
93	4	11	141	Dump tank	4" top blind hub
94	4	12	142	Dump tank	4" hub bottom butt weld
95	4	13	45	Test vessel	2" hub N
96	4	14	46	Test vessel	1" bottommost hub
97	4	15	47	3/4" line	below test vessel, bottom curve
98	4	16	48	3/4" cleaning line	bottom
99	4	17	143	Dump tank	2" hub
100	4	18	145	1/2" drain line	bottom
101	4	19	146	1/2" drain line	middle
102	4	20	148	1/2" drain line	top
103	4	21	150	Nozzle	at tip
104	4	22	152	1/4" CO_2 line	fluid temperature near nozzle
105	4	23	151	1/4" CO_2 line	near nozzle
106	4	24	Empty	Empty	
107	4	25	Empty	Empty	
108	4	26	Empty	Empty	

109	4	27	Voltage0	Level indicator for dump tank	6" above bottom of tank
110	4	28	Voltage1	Level indicator for test vessel	15 inches above nozzle
111	4	29	Voltage2	Level indicator for dump tank	0.5" above bottom of tank
112	4	30	Voltage3	Level indicator for dump tank	4" above bottom of tank
113	4	31	Voltage4	Empty	
114	2	-	Current0	Flow rate Argon/CO_2 (QMBM 3)	
115	2	-	Current1	Density Argon/CO_2 (QMBM 3)	
116	2	-	Current2	Empty	
117	2	-	Current3	Empty	
118	-	-	RS485_0	Cover gas (Argon) flowrate (HFC-D-301)	
119	-	-	RS485_1	Argon nozzle flowrate (HFM-D-302)	
120	-	-	RS485_2	Empty	
121	-	-	RS485_3	Empty	
122	-	-	Serial_0	Laser level meter	Test vessel
123	-	-	Ethernet_0	Pressure 1, Test vessel	Top of test vessel
124	-	-	Ethernet_1	Pressure 2, CO_2	Near reservoir

Sodium loading

Approximately 44 lbs (20 kg; ~21 L/5.5 gal) of sodium were transferred into the SNAKE dump tank on July 19, 2012. This sodium came from a clean sodium storage drum that Argonne has had on site since 1989 (see photo in Figure 1). A 3/8 inch line extends from the sodium storage drum, which was hooked up to the ¾ inch fill port on the dump tank. The sodium storage tank was heated to 110 ˚C, while the dump tank and transfer tubing were heated to 119 ˚C. While the melting and self-ignition temperatures of sodium are 97.72 ˚C, and 120 ˚C, respectively, the transfer temperatures listed above have been tuned by Argonne researchers over a number of decades with great success. It is particularly important to avoid the chance of plugging in the transfer tubing since removing a plug could be difficult depending on the presence of contaminants.

Prior to the transfer of sodium, several precautions were taken in order to reduce and mitigate sodium fires. First, the sodium scrubber system was fully prepared for service. This involved some maintenance which included cleaning of the Venturi nozzles, flushing of the magnehilic differential pressure gauges, and checkout of the whole system. A drum of dry silica sand and a MET-L-X fire extinguisher were placed near the SNAKE facility for emergency fire suppression preparedness. During the transfer, the operators donned flame retardant clothing (long-sleeved shirt & pants, fire-suit), safety shoes, chemical goggles, leather spats, gauntlet-style chrome leather welding gloves, and hard hats with face shields. The Argonne Fire Department was alerted of the procedure.

Once these preparations were made, a rough vacuum of under 0.75 mbar (75 Pa; 0.6 mm Hg) was drawn on the sodium dump tank, pulled through a sodium separator packed with stainless steel wool to prevent sodium vapor from entering the vacuum or clogging the line. A vacuum was used to "pull" the sodium into the dump tank because it avoids having an open vent which would expose the sodium to oxygen. A slight overpressure (3 psi) of dried Ultra High Purity (UHP) argon (<2 ppm water, <2 ppm oxygen) was maintained on the sodium storage drum in order to avoid contamination. The sodium drum was placed on a digital scale in order to monitor the drum weight change and estimate the mass of sodium transferred. Three conductivity probes were inserted from the top of the dump tank at several heights (1inch, 4 inch, and 5.8 inch from tank bottom) to monitor the sodium level. The dump tank was isolated from the vacuum to reduce the opportunity for sodium vapor leakage and then all valves between the sodium transfer drum and dump tank were opened. The weight scale and conductivity level probes were used to monitor the transfer, and the valves between the two tanks were closed once the target level was reached. All systems were allowed to completely cool to room temperature. The dump tank was then back-filled with UHP argon to ~10 psi. The transfer tubing was carefully removed and all open tubes were capped. The capped transfer tubing and sodium storage drum were then placed in a sodium storage room.

Miscellaneous activities

Additional activities carried out in FY 2012 that were not listed above but are worthy of mention are outlined below. This list provides a nearly complete picture of the facility construction status as of the writing of this report.

- Significant resources were devoted toward making the safety case for the SNAKE facility by both the SNAKE experiment staff and the ANL Nuclear Engineering Experiment Safety Review Committee (ESRC). The initial safety writeup document was prepared during January 2012, and formally submitted to the review committee on February 9, 2012. After a lengthy review process requiring a number of revisions to the document and procedures, the full experiment safety program for SNAKE was approved on June 25, 2012. This process included formal safety reviews by two pressure safety Subject Matter Experts (SME) and one Asphyxiant Gas/Toxic Gas SME. Several of the new safety analyses and procedures are included in Section 4 of this report. Standard Operating Procedures (SOPs) were developed as part of this

process. These include pre-experiment sodium transfer and vessel heat up, experiment, normal shutdown, emergency shutdown, and pressure testing procedures.

- Connection of the experiment enclosure to the Building 206 Alkali Metal Passivation Booth (Scrubber) was completed. This work consisted of installing a booster fan on the outside of the enclosure and a duct system extending from the enclosure, through a wall, to the scrubber. This work was done under the supervision of Argonne Health Physics since the scrubber and associated pipes are radioactively contaminated. This activity included removal and replacement of contaminated duct work near the scrubber.
- All vessels and components were installed in the enclosure.
- The mass spectrometer was calibrated in-house using calibration gases of specific mixtures of argon and carbon dioxide. The mass spectrometer was mounted on the outside of the SNAKE facility (see Figure 12).

Figure 12: Mass spectrometer mounted on outside of SNAKE facility. The duct that runs to the scrubber is pictured at the top, while two wire terminal boxes that contain the heater controller wires are located above the mass spectrometer.

- The building power (120V) was upgraded around the experiment facility. This included additional circuits and outlets along the high-bay walls, and on both the exterior and interior of the SNAKE enclosure. Permanent lighting was also included inside the enclosure.

- Power wiring to the sodium-component heaters (heater cables and heater tape) was installed, as well as heater control wiring and thermocouples to the temperature controllers. Low temperature (~200 ˚C) testing of all components was completed. See Figure 13 for a photograph of the heater tape wrapped around the tubing and valves that run between the test section and dump tank.

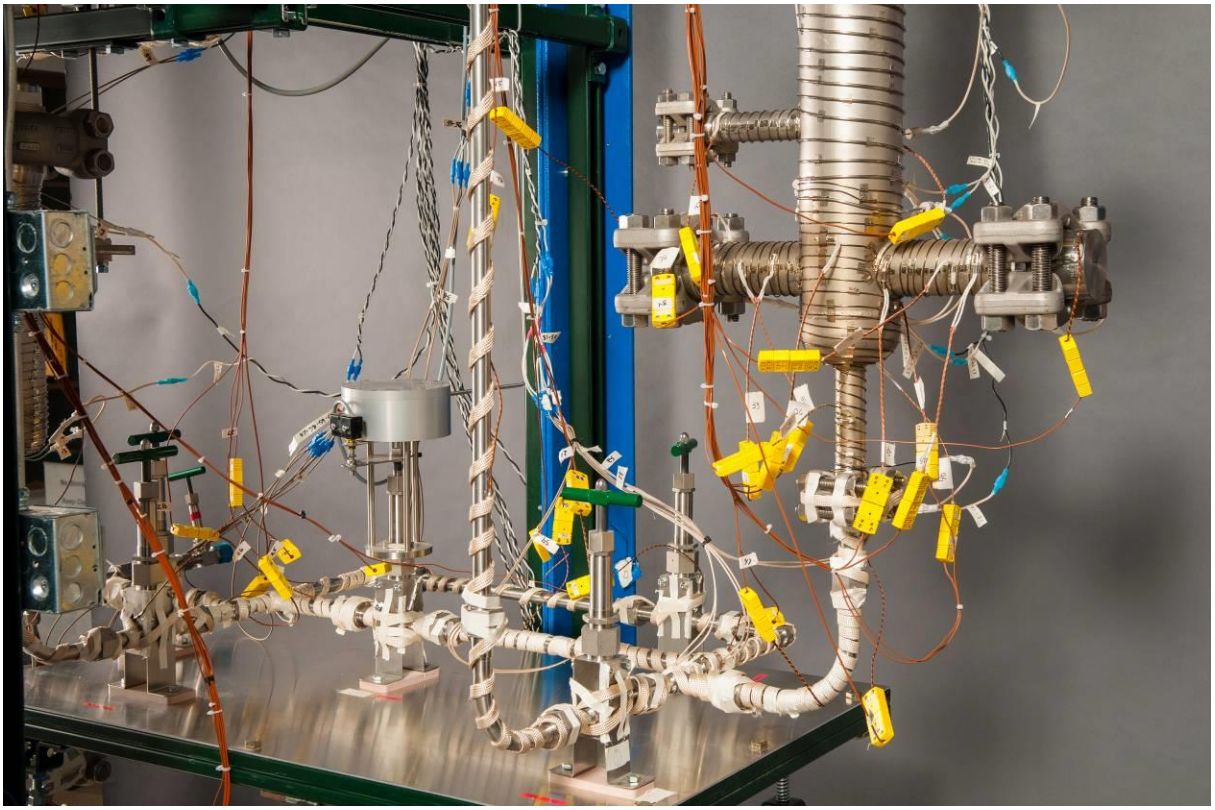

Figure 13: Heater tape wrapped around the tubing and valves that run between the test section (top right) and dump tank (not pictured – bottom left). The emergency dump valve is located in the center of the photograph.

- Installation of the Grayloc® flanges to the large-diameter fittings was completed, which included torqueing to the manufacturer suggested values.
- The cover gas control system was assembled and connected to the sodium system.
- Building air was connected to the sodium pneumatic valves (emergency and drain) through a solenoid control system.
- Installation of the cold trap and separator were completed. This involved the addition of single-strand stainless steel wool to both.
- The exhaust line of the facility was run outside of the high bay in order to ensure asphyxiant and toxic gases generated by the experiment.
- A custom instrument power supply and control panel rack mount was installed and has been tested (see Figure 14 for photograph).

- Design and wiring of the automatic safety system has begun. It is anticipated that completion of this system will occur between September-October 2012.
- A rack-mount control panel for the pneumatic valves has been assembled (see Figure 14 for photograph) and tested. This system allows for manual or automatic (LabView) valve control.

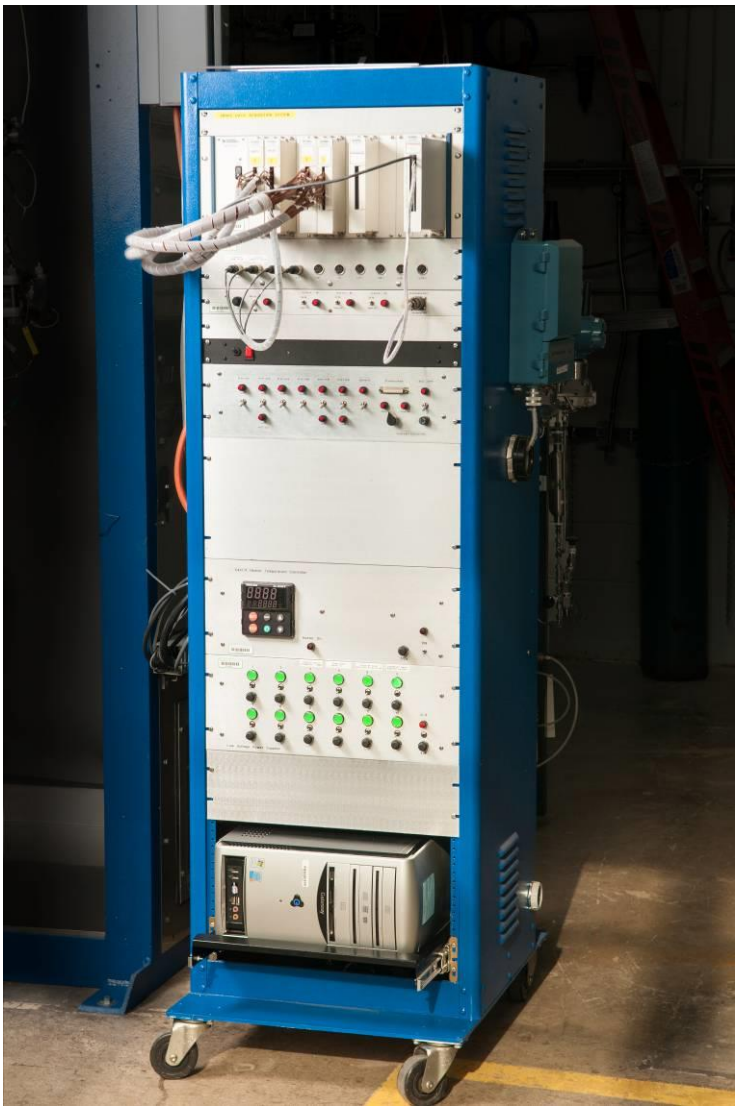

Figure 14: Control rack with National Instruments chassis on top, valve control panel in the middle, and instrument power near the bottom.

- All pressure relief devices have been installed. Several of these devices are adjustable relief valves that were calibrated in-house.
- The full sodium system has passed pressure and vacuum tests.
- Additional heaters have been added to flanges and other critical components. Initial heatup was completed of the entire system to 200 ˚C for at least an hour. Little insulation has been placed around the test vessel and related components in order to

allow for easy inspection during the initial tests and simplify the system. This will limit the initial experiments to a temperature of approximately 200 ˚C. Further high-temperature tests will be carried out in FY 2013 after the insulation has been installed.

- Several gas leaks were found in the sodium system, primarily from the multi-junction thermocouples. Most of these leaks have been fixed. They were found by using the mass spectrometer installed on the system after pressurizing components to a few psi of argon.
- Installation of sodium-spill redirection plates on the enclosure doors was completed and was a safety requirement prior to testing.
- Attempts to prepare the laser level probe for monitoring the test vessel sodium height have been unsuccessful and will not be continued until FY 2013. A backup single-conductor conductivity probe was assembled to provide an indication of filling for the first experiments. This continuity probe was suspended in the test vessel and reaches 38.1 cm (15 inch) above the nozzle.
- Assembly of the first two test nozzles has been completed and passed hydrostatic pressure testing. The first nozzle assembly was installed in the test vessel (see Figure 15).

Figure 15: Nozzle and gas line installed on test vessel.

- Permanent installation of a vacuum pump was completed to easily facilitate pump-down of either the test vessel or dump tank (see Figure 16)

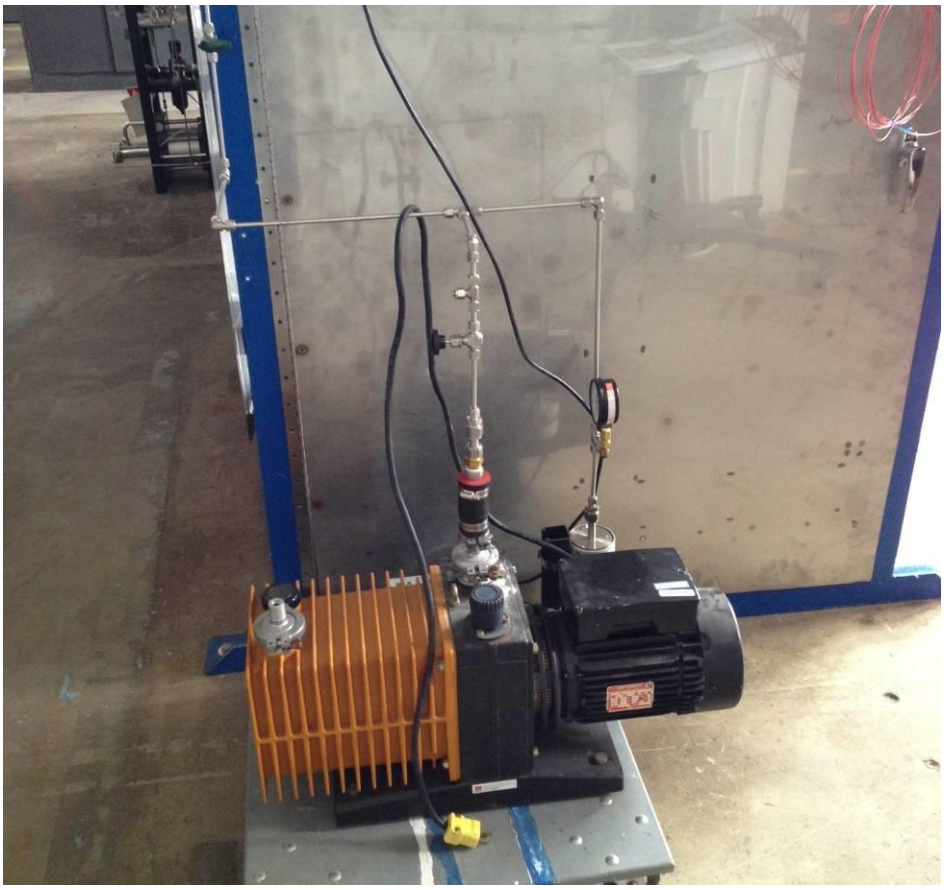

Figure 16: Permanent installation of vacuum pump to facilitate pump-down of either test vessel or dump tank.

The assembled state of the facility as of the writing of this report is shown in Figure 17.

Figure 17: Assembled state of the SNAKE facility as of September 2012 (4 front doors are open to view interior).

4 Shakedown Tests and Data

A number of shakedown tests were completed to begin the process of verification of equipment and to refine operational parameters and procedures. These tests are summarized below.

Gas system blowdown into water

The first major experimental activity carried out with the SNAKE facility was to shakedown the entire gas system including argon nozzle purge, pressurization of the CO_2 line, and blowdown of S-CO_2 into a tank of water. The glass vessel that contained the water is shown in Figure 18 with a micro-nozzle assembly installed in it. The micro-nozzle faces upwards as it does in the sodium test vessel. The water tank setup allows for visualization of the blowdown of gasses through a micro-nozzle into a sodium surrogate liquid.

Figure 18: Glass tank with micro-nozzle assembly installed. This tank can be filled with water which allows for visualization of the blowdown of S-CO_2 into a fluid.

A picture of S-CO_2 blowdown into water through the micro-nozzle is shown in Figure 19. From this image, it is possible to see that the CO_2 jet spreads from the micro-nozzle diameter of 65 µm to approximately 12.94 cm at a height of 18 cm above the tip. While the behavior in sodium would be somewhat different, this test gives a rough idea of what the jet will look like in sodium since the hydraulic properties of water and molten sodium are fairly similar.

Figure 19: Supercritical CO_2 at 7.8 MPa sparging into water from a micro-nozzle assembly

In addition to enabling visualization of the jet blowdown, this shakedown test also made it possible to verify that the valves, flow meters, CO_2 pre-heater, and booster pump functioned properly. Several gas line improvements and modifications to the DAS were made as a result of the shakedown tests. These tests also showed that the booster pump can successfully pressurize the CO_2 above the critical pressure of 7.39 MPa (1070 psi), and that the pump can maintain pressure in the line during steady-state blowdown through the micro-nozzle.

Test vessel filling with sodium checkout

The ability to fill and drain the test vessel was evaluated. The test vessel had a 10 slpm flow of argon cover gas and a slight argon purge was maintained through the micro-nozzle. This kept the test vessel at slightly above atmospheric pressure, approximately at 115 kPa (2 psig). A valve at the exhaust was kept partially closed to enable this slight overpressurization. The dump tank was isolated from the rest of the system and then pressurized to approximately 136 kPa (5 psig). The test vessel and dump tank were maintained at approximately 170 ˚C and 115 ˚C, respectively. The manual valve, MV-SOD-01, was opened to allow sodium to flow from the dump tank into the test vessel. A single continuity probe, or level probe, extended from the top of the test vessel to 38.1 cm (15 inch) above the micro-nozzle. When sodium made contact with the probe, current was able to pass through the probe and sodium to ground which was read as a closed circuit. This is shown in Figure 20 as the solid black line where a value of 20 represents the circuit being closed, thus sodium has reached the level probe, and a value of zero represents the circuit being open meaning sodium is below the probe. Sodium clearly impacts the level probe at approximately 1000 seconds and is removed from the probe at approximately 6800 seconds.

Temperature data from several of the bottom thermocouples of the thermocouple rake suspended inside of the test vessel are shown in Figure 20. The thermocouples located at 1.7 inches and 11.7 inches above the micro-nozzle exhibit a clear dip when the cool (115 ˚C) sodium wets each thermocouple location at approximately 1000 seconds. The thermocouple at 21.7 inches above the nozzle shows no dip, demonstrating that the sodium level did not reach that height. It takes approximately 1000 seconds for the sodium temperature to heat up to the original test vessel temperature.

The temperature data is not able to demonstrate sodium draining as neither the dump tank probes nor thermocouple probes show any substantial temperature changes when the sodium is drained at 6800 seconds. While this is unsurprising for the test vessel data, it was hoped that some increase in the dump tank temperature would be observed. The increase in dump tank temperature at approximately 4800 seconds is due to the operators manually increasing the dump tank heater power to ensure that there was no freezing in either the dump tank or drain lines.

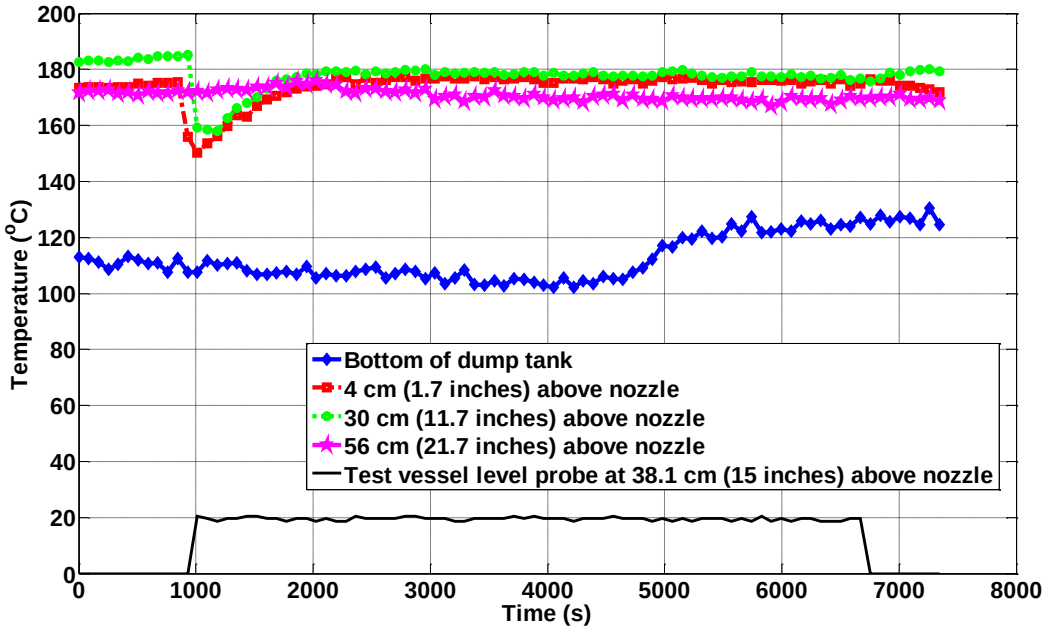

Figure 20: Temperatures of select dump tank and test vessel rake thermocouples during sodium filling of the test vessel.

First fundamental sodium-CO_2 interaction experiment

The first fundamental sodium-CO_2 interaction experiment to take place at Argonne occurred on September 19th, 2012. Approximately 247 grams of CO_2 (125 standard liters) were injected into the sodium pool over the course of 30 minutes. The flow rate in g/hr and slpm along with the measured density from the Coriolis flow meter are all shown in Figure 21. The Coriolis flow meter directly measures mass flow rate in g/hr and the gas density. The equivalent flow rate in standard liters per minute can be found simply as:

$$\dot{V}(slpm) = \dot{m}(g/hr)/1000/60*1.977(g/L)$$

where the value 1.977 g/L is the density of CO_2 at standard conditions. The total injected amount of CO_2 is simply found by finding the area under the mass flowrate curve, in this case using the trapezoidal numerical integration method.

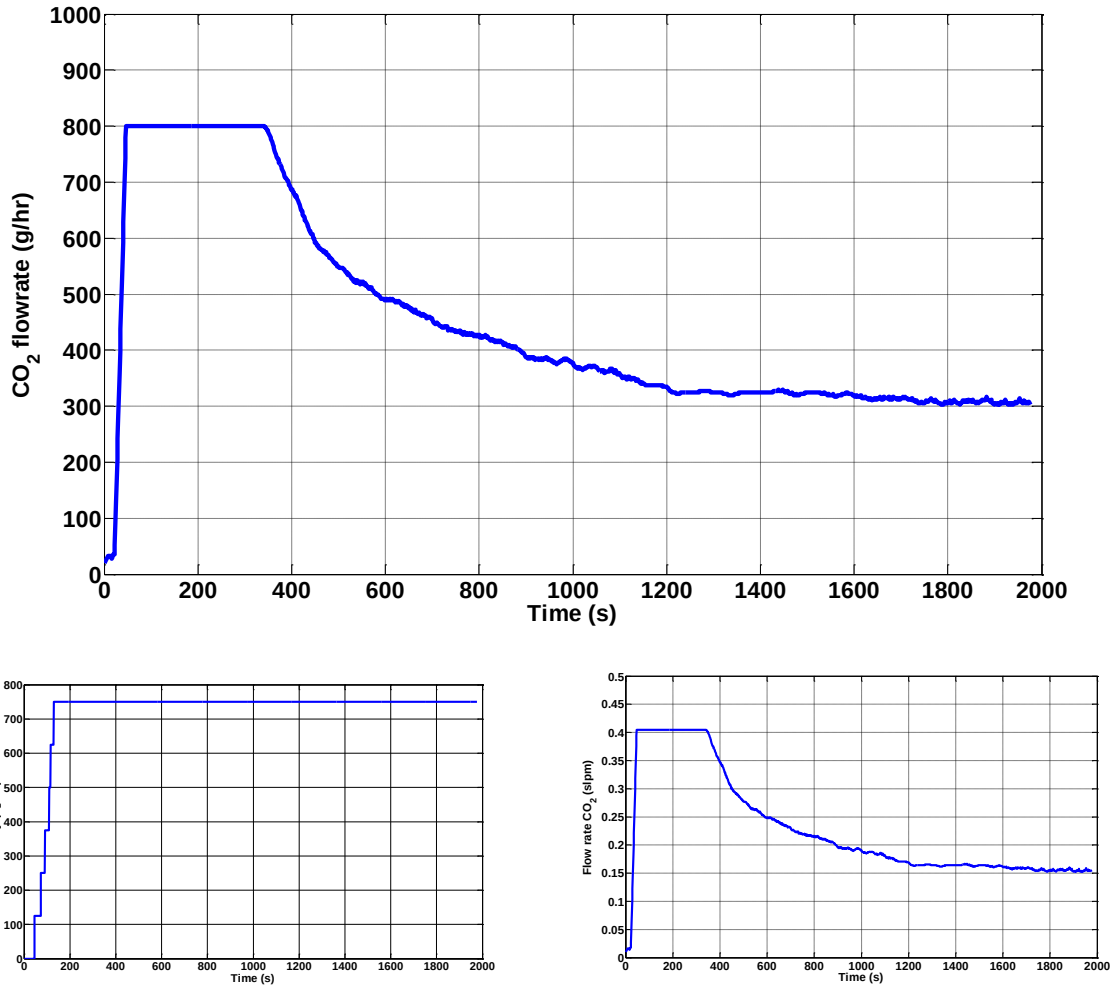

Figure 21: Measured CO_2 flow rate through the Coriolis flow meter in g/hr (top). Measured gas density (left) and conversion to standard liters per minute (right). A moving average was used to clean up the curve and remove noise.

The mass flow rate quickly ramps up to approximately 800 g/hr for the first 350 sec of injection and then slowly levels out to approximately 300 g/hr. After the valve PV-02 is open at time=0 sec, there is a slight depressurization in the CO_2 reservoir, which started at 9,132 kPa, as CO_2 rushes in to the ¼ inch line between PV-02 and the micro-nozzle (as shown in Figure 22). This represents several meters of line that was maintained only at approximately 789 kPa (100 psig); thus, there is a substantial volume to fill and equalize the pressure with the reservoir. The pressure in the reservoir dips to 7,440 kPa at 145 sec which is just slightly above the supercritical pressure. The pressure then re-stabilizes above 9,000 kPa (1300 psi) by 1000 sec. It should be noted that the mass flow rate behavior is significant in that the flow rate does not reduce beyond the initial spike caused by the in-rush through the nozzle line of CO_2. Some researchers had expected that the chemical reaction between sodium and CO_2 would cause solid products to accumulate and plug the micro-nozzle. If this had happened, then the flowrate would have continued to fall further rather than level off at approximately 300 g/hr.

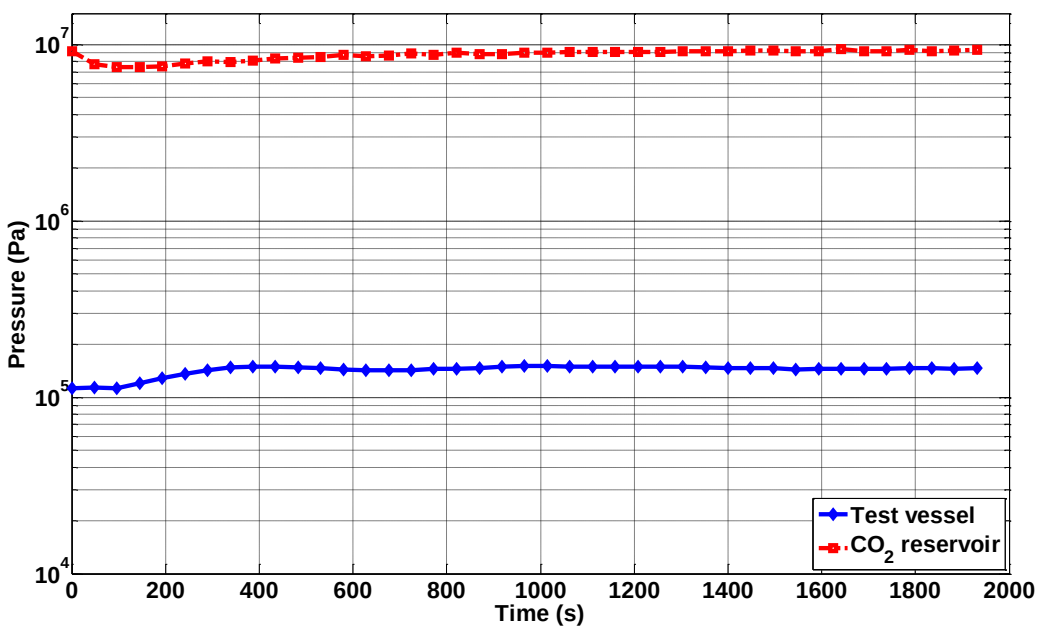

Figure 22: Pressures of the test vessel and CO_2 reservoir.

The CO_2 nozzle temperature during this first test is shown in Figure 23. The nozzle temperature is kept fairly constant at approximately 170 ˚C. It starts at 165 ˚C with a gradual increase to 175 ˚C after 800 seconds and then a gradual decrease back to 165 ˚C by 2000 seconds. It was somewhat surprising that there was not a slight increase in nozzle temperature at the beginning of CO_2 injection or a decrease throughout the injection process. This would be expected since the CO_2 pre-heating is not controlled perfectly and is dependent on the CO_2 properties as it flows through the pre-heater, also shown in Figure 23. Initially, the CO_2 flow rate is very high through the pre-heater as the line between the PV-02 and the micro-nozzle pressurizes, which means heat transfer is very good through the pre-heater and the CO_2 temperature increases to a peak at 70 s. This behavior is not reflected at the nozzle

tip. Isentropic expansion through the nozzle should also decrease the nozzle temperature. The lack of any significant temperature change could mean that the thermocouple located near the nozzle tip is actually in contact with the stainless steel rather than suspended in the fluid flow. The temperature of the stainless steel is more stable than the gas temperature across any transient. Assembly of future nozzle systems should take this into account and make an effort to avoid contact of the nozzle thermocouple with the stainless nozzle walls.

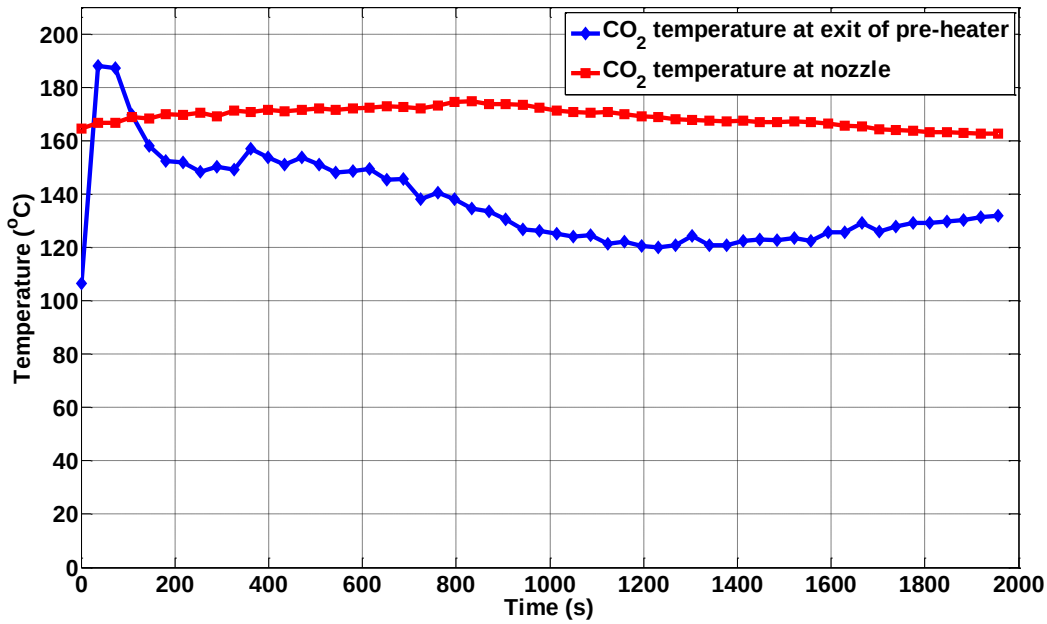

Figure 23: Nozzle temperature during first sodium-CO_2 test

The temperatures measured at several thermocouples along the thermocouple rake are shown in Figure 24. The bottom thermocouple, at 4 cm above the nozzle tip, exhibits a steady temperature profile similar to the nozzle tip temperature that was shown in Figure 23. This further suggests that the nozzle thermocouple is in contact with the nozzle tip wall, thus measuring the sodium temperature rather than the CO_2 temperature. The other interesting behavior is the spikes in temperature seen in the thermocouples at 30 cm and 43 cm above the nozzle at 400 sec and 600 sec, respectively. It is unclear why the temperature would spike at these locations. It could mean that there is some splashing of sodium as CO_2 is injected and sparges through the sodium pool. This behavior will have to be monitored in future tests to narrow down what is happening. The addition of a better level detection method that can monitor the sodium pool height change would potentially help understand the source of the temperature spikes.

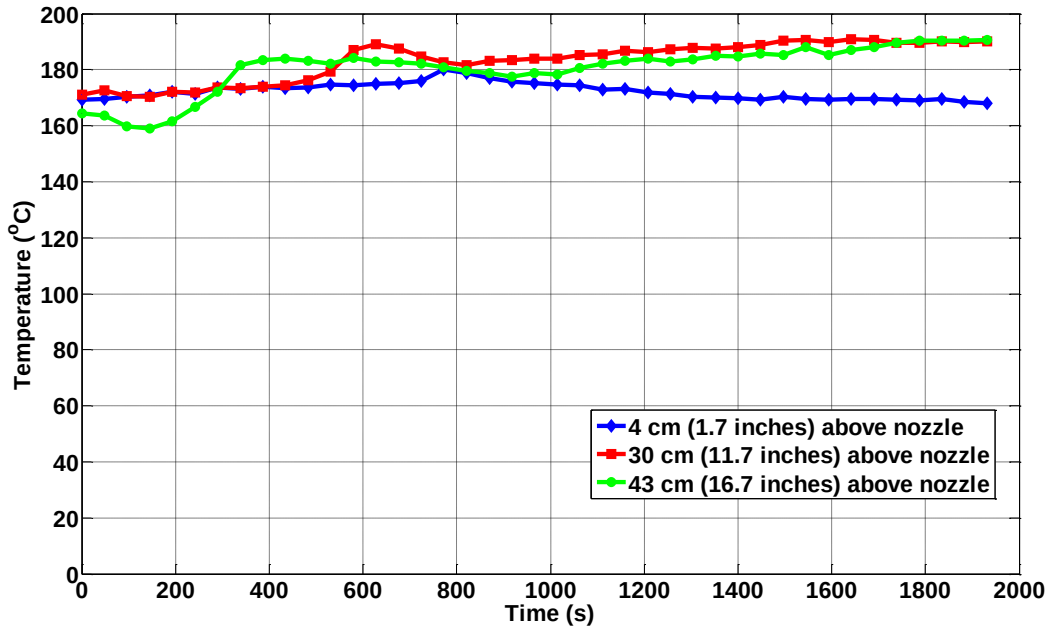

Figure 24: Thermcouple rake temperatures during first sodium-CO_2 test. A moving average was used to clean up the curve and remove noise.

The raw data from the mass spectrometer is shown in Figure 25. A test was completed prior to the first sodium fill of the test vessel at approximately the same conditions as the first sodium-CO_2 interaction test. In other words, the test vessel temperature was kept at approximately 170 ˚C with and without sodium. The CO_2 injection pressure was maintained at approximately 9,000 kPa in both cases. The only significant difference between the two tests is the presence of sodium in the second case. The test without sodium acts as a control case for the mass spectrometer and any significant differences in gas detection between the two tests can be attributed to the interaction between sodium and CO_2.

It takes approximately 200 seconds from the time the switch in nozzle injection from argon to CO_2 is made at SV-02 and the time that CO_2 is detected at the mass spectrometer. This is the characteristic flow time lag. It is quite substantial because of the long path the CO_2 takes through the injection line, pre-heater, test vessel, and exhaust line before it finally encounters the capillary that carries small amounts of the exhaust gas to the mass spectrometer for analyzing. There may be some delay also due to the switch over between argon and CO_2 when argon is compressed toward the micro-nozzle. Very little mixing of argon and CO_2 would be expected in the injection line. So the argon inventory in the line has to be nearly depleted through the micro-nozzle before CO_2 could begin to be released. The flow through the nozzle is choked, so it takes quite some time for the gas to pass from the switch-over valves (PV-02 & PV-03) and into the test vessel.

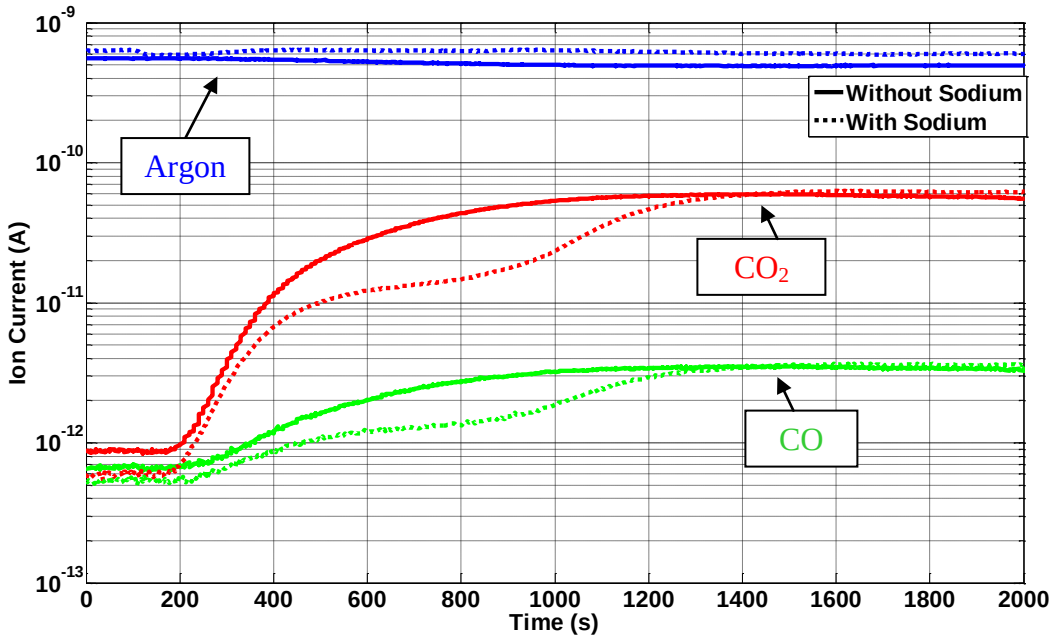

Figure 25: Raw mass spectrometer data comparing the relative peak heights of argon, carbon dioxide and carbon monoxide for two tests. Solid lines represent a test where carbon dioxide was vented through the micro-nozzle into the empty heated test vessel. Dotted lines represent a test where carbon dioxide was vented through the micro-nozzle into the test vessel under comparable conditions with the addition of sodium being present in the vessel.

The mass spectrometer analyzes residual gases by ionizing some of the gas molecules flowing through the exhaust line of the SNAKE experiment, and separating the resulting ions according to their respective masses. The ion currents are measured at each mass. When the gases are ionized by the high energy electrons in the ionizer, some molecules will be split into pieces, called fragments. Each molecule has a typical fragmentation behavior, or cracking pattern. For example, carbon dioxide will crack into fragments of CO, C, and O in a specific ratio. The cracking pattern for carbon dioxide is shown in Table 3 with the highest peak (CO_2) normalized to 100. From these cracking patterns, it can be seen that there will be some carbon monoxide detected even when pure CO_2 is passed through an empty vessel, which is the behavior detected in Figure 25.

Table 3: Standard Cracking Patterns for CO_2 and CO. Highest Peak Normalized to 100

Mass number	CO_2	CO
44	100	-
28	10.99	100
16	8.99	2.00
12	6.01	4.99

It is unclear why the detected ion intensity of CO_2 and CO is lower when sodium is present from time 200 sec to approximately 1200 sec. The data with sodium present has an inflection point at approximately 900 seconds where the ion currents start increasing again. This behavior was not seen when no sodium was present and is not expected. A number of

additional tests will need to be completed in order to verify that the presence of sodium is the cause of the observed behavior, and that it is not due to differences in the initial conditions of the two tests. The later situation is what the researchers currently believe is the explanation, but further testing will be completed in early FY 2013 to investigate this behavior. It is possible, but unlikely, that sodium actually slows the release of gases to the significant extent exhibited in Figure 25.

The primary objective of the mass spectrometer measurements of the exhaust gas is to detect gaseous reaction products released by the interaction between CO_2 and sodium. Previous researchers have detected CO under certain reaction conditions. Since CO is detected by the mass spectrometer as a fragment in even a pure CO_2 environment, it is difficult to clearly determine the presence of reaction products in the exhaust line. In order to show the relative presence of CO compared with CO_2, the ratio of M_{44} to M_{28} is plotted for the two tests in Figure 26. Lower values of this ratio mean that a greater fraction of CO is detected by the mass spectrometer. The ratio quickly jumps to a nearly steady state value of approximately 21 in the test without sodium. This step-change behavior is expected since the cracking ratio is a fixed property of the gas/spectrometer combination. However, a value of 21 is quite high. The ratio expected is closer to 9.1 according to the cracking pattern in Table 3. It is unclear what the cause of the high steady-state ratio is. More investigation into this issue will take place in FY 2013 including additional calibration and mass spectrometer tuning activities.

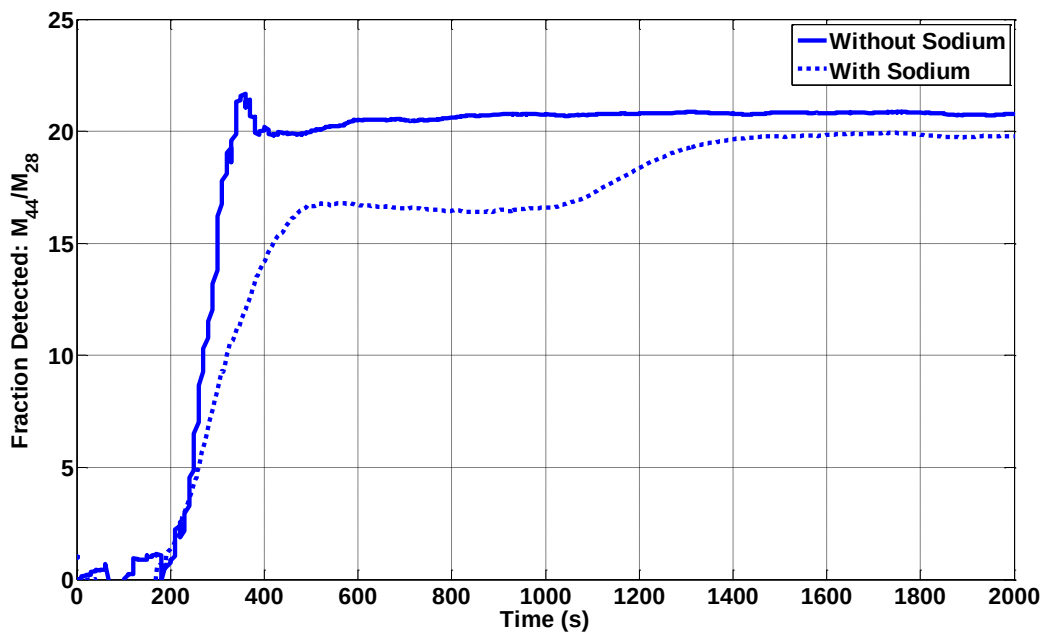

Figure 26: Fraction of Mass 44 (CO_2) divided by Mass 28 (CO) detected. A moving average was used to clean up the curve and remove noise.

The ratio of M_{44} to M_{28} for the test with sodium does have a slightly different behavior than for the test without sodium. Surprisingly, there is not a dramatic step change after

injection, like there was without sodium. The "with sodium" curve is below that of the test without sodium at all times, which would imply that there is, in fact, a chemical reaction occurring since more CO is detected than would be expected due solely to cracking of CO_2. However, the data with sodium behaves oddly. The ratio levels out at 16 at 500 sec before increasing again at 1000 sec. This suggests that either there was a change in the chemical reaction between carbon dioxide and sodium at 1000 sec, or that there is a partial pressure dependence on the ratio that should not exist.

At this time, it is not clear what the discrepancies are in a) the magnitude of the M_{44} to M_{28} ratio or b) partial-pressure dependence of the ratio. A cursory glance at the data would suggest that there was CO production from the interaction between sodium and CO_2. However, due to the discrepancies mentioned, the production of CO is ambiguous. Data collection and interpretation will need to be improved. This can happen when additional experiments are run, the mass spectrometer has been further calibrated, and through the addition of a dedicated CO detector on the exhaust line that uses a different measurement technique than the mass spectrometer. It should also be noted that the production of carbon monoxide at the test temperature completed here (170 ˚C) is not necessarily expected. Other researchers (Eoh et al., 2010) have not seen substantial reaction products until a temperature of 300 ˚C. This is an additional reason for skepticism that CO was generated during this first test.

5 Lessons Learned from the First Test and Future Work

A number of lessons were learned from the first set of shakedown tests, including:

1. The mass spectrometer has a difficult time clearly measuring the generation of carbon monoxide when compared with the cracking pattern of carbon dioxide. Additional calibration activities are required and the addition of a dedicated carbon monoxide detector on the exhaust line is recommended.

2. The continuity-type level detectors that are often used in liquid metal facilities are plagued with problems. Namely, there exists the possibility that sodium vapor could accumulate up in the vessel head and then condense near the fitting supporting the continuity probe. This phenomenon is called sodium frost, and can cause false-shorting of the probe. It is desired to have a better method of level detection that includes the capability of monitoring the height at any point in the vessel with a single detector.

3. Additional methods of monitoring sodium flow and location are desired. The inclusion of electromagnetic (EM) sodium flow meters would help greatly.

4. Direct measurement of the exhaust flow rate would enable improved reaction product mass balances.

5. Trace heating and insulation can be improved in a number of lines to enable better temperature control and smaller temperature gradients.

There are a number of activities planned for FY 2013 and beyond. Some of these are listed below; however, not all of these items will be carried out due to time and funding restrictions. These activities should be carried out in addition to, but before, execution of the planned text matrix for FY 2013.

1. Calibrate the mass spectrometer and verify calibration with several known combinations of argon/CO_2/CO.

2. Add a dedicated CO detector to exhaust line.

3. Add a mass flow meter to exhaust gas line.

4. Add a compressor to the air side of the gas-booster in order to eliminate quick discharge of air gas bottles that currently provide boost pressure.

5. Improve heating and insulation of trace heated sodium lines.

6. Clean and replace level probes in the test vessel.

7. Add an additional whole-vessel level probe.

8. Purchase a hand-held density detector to locate sodium plugs and location.

9. Add a pump and flow meter to the sodium line to monitor flow and add an automatic cleanup capability.

10. Improve cold trap and filter temperature control.

11. Improve LabView data acquisition recording and display.

12. Add mock PCHE channel to tip of nozzles to test representative geometry.

13. Further analyze data from the first experiment to quantify CO production, if any.

14. Improve placement of nozzle thermocouples to ensure measurement of fluid temperature and avoid measurement of wall temperature.

6 Summary

One appealing feature of the supercritical carbon dioxide Brayton cycle energy conversion system is the small footprint that the hardware requires, which is in part due to the use of Printed Circuit Heat Exchangers (PCHEs) as the heat source heat exchanger (sodium-to-CO_2) as well as the recuperator and cooler modules. Although PCHEs have a high degree of structural integrity, the potential for leaks to develop between the sodium and CO_2 coolant channels in the secondary heat exchanger cannot be ruled out, and this would lead to discharge of high pressure CO_2 into the secondary coolant circuit. Due to the robustness of the PCHE design, catastrophic failure leading to CO_2 jet blowdown into the secondary sodium loop is not deemed likely. Rather, small cracks (or micro-leaks) may develop in which CO_2 will bleed into the secondary system at a relatively low rate and chemically react with the sodium.

The goal of the sodium-CO_2 interaction tests is to gain a fundamental understanding of sodium-CO_2 interactions under prototypical conditions of compact diffusion-bonded heat exchanger failure, a fundamental understanding of self-plugging if it occurs, and the development of one-dimensional phenomenological models for the interactions between high-pressure CO_2 issuing into liquid sodium from a micro-leak across a stainless steel pressure boundary. These models will be validated using experiment data.

Therefore, an experiment program at Argonne was initiated in FY 2010 to investigate the reaction characteristics between sodium and CO_2 under micro-leak conditions. A deliverable report described the facility scaling rationale and design. Assembly of the SNAKE (S-CO_2, Na Kinetics Experiment) began in FY 2011 and was completed in July 2012. Approximately 44 lbs (20 kg; ~21 L/5.5 gal) of sodium was transferred into the SNAKE dump tank from a drum of clean sodium on July 19, 2012.

The first sodium-CO_2 interaction experiment was carried out at SNAKE in September 2012. This test was successful in that supercritical carbon dioxide was sparged into a pool of sodium through a 64 µm diameter nozzle. Approximately 125 standard liters of CO_2 were injected into a 38.1 cm (15 inch) high column of sodium at 170 ˚C over the course of 30 minutes at a pressure of approximately 9.0 MPa (1300 psi). This is the first known test involving supercritical CO_2 and sodium. Preliminary data analysis suggests that a small amount of carbon monoxide was produced from the reaction between sodium and CO_2. No plugging of the micro-nozzle was detected during this experiment. Further analysis is required prior to unequivocally stating that CO was produced in this test. More detailed analysis of this set of data and planning for improving data quality and facility control will take place in early FY 2013.

Fiscal Year 2013 will involve formulating a sodium-CO_2 interaction test matrix to be delivered in April 2013, making additional hardware improvements to improve data quality, executing the test matrix, and preparing a detailed report to be delivered in September 2013. A number of lessons were learned from the first shakedown experiment, which has led to suggested facility improvements. These improvements will also take place in FY 2013.

Model development and validation are planned for the following Fiscal Year, with a detailed model report anticipated to be delivered in September 2014.

References

1. Advanced Reactor Concepts (ARC) Fact Sheet, U.S. Department of Energy's Office of Nuclear Energy, http://www.nuclear.energy.gov/pdfFiles/factSheets/2012_AdvReactor_Factsheet_Final.pdf, Accessed September, (2011).
2. ASHRAE: *Systems Handbook*, (1980).
3. J.E. Brockman, F.E. Arellano, and D.A. Lucero, "Validation of Models of Gas holdup in the CORCON Code," NUREG/CR-5433, SAND89-1951, Sandia National Laboratories, December, (1989).
4. Y. Chang, P. Finck, C. Grandy, "Advanced Burner Test Reactor Preconceptual Design Report," September 5, 2006, ANL-ABR-1/ANL-AFCI-173, (2006).
5. M. Denman, J. LaChance, T. Sofu, G. Flanagan, R. Wigeland, and R. Bari, "Sodium Fast Reactor Safety and Licensing Research Plan - Volume 1," SAND2012-4260, Sandia National Laboratories, May (2012).
6. J.H. Eoh, H.C. No, Y.H. Yoo, J.Y. Jeong, J.M Kim, S.O. Kim, "Wastage and Self-Plugging by a Potential CO_2 Ingress in a Supercritical CO_2 Power Conversion System of an SFR," J. Nuclear Science and Technology, Vol. 47(11), pp. 1023-1036, (2010).
7. M.T. Farmer, D.J. Kilsdonk, J.J. Sienicki, and C. Grandy, "Design of a Test Facility to Investigate Fundamental Na-CO_2 Interactions in Compact Heat Exchangers," ANL-GENIV-164, (2010).
8. J. Fink, L. Leibowitz, "Thermodynamic and Transport Properties of Sodium Liquid and Vapor," Argonne National Laboratory, ANL/RE-95/2, (1995).
9. C. Gerardi and C. Youngdahl, "Sodium-Water Reaction Analysis Code SWAAM-II Recovery and Development Efforts," ANL-GenIV-172, September, (2010).
10. C. Gerardi, M.T. Farmer, D.J. Kilsdonk, J.J. Sienicki, and C. Grandy, "Fundamental Na-CO_2 Interactions in Compact Heat Exchangers Experiment (SNAKE): FY 2011 Status Update," ANL-ARC-199, (2011).
11. C. Gerardi, M.T. Farmer, D.J. Kilsdonk, J.J. Sienicki, and C. Grandy, "Na-CO_2 Interactions Experiment (SNAKE): FY 2012 Update on Facility Assembly and Sodium Loading," ANL-ARC-290, (2012).
12. L. Gicquel, C. Latgé, and N. Simon, "Supercritical CO_2 Brayton Cycle Coupled with a Sodium Fast Reactor: Na/CO_2 Interaction Experiments and Modeling," Paper 10215, 2010 International Congress on Advances in Nuclear Power Plants (ICAPP '10), San Diego, CA, USA, June 13-17, (2010).
13. L. Gicquel, C. Latgé, and N. Simon, Ph. Hobbes, A. Soboni, J.C. Buvat, J.L. Gustin, "Brayton Cycle with SC-CO_2: Investigations of Sodium-Carbon Dioxide Interactions," Slides from Meeting with A. Moisseytsev (ANL), April 27-29, (2011).
14. I. Kataoka and M. Ishii, "Mechanistic Modeling and Correlations for Pool Entrainment Phenomenon," Int. J. Heat Mass Transfer, Vol. 27, pp. 199-2014, (1984).

15. X. Li, R. Le Pierres, and S. J. Dewson, "Heat Exchangers for the Next Generation of Nuclear Reactors," Paper 6105, 2006 International Congress on Advances in Nuclear Power Plants (ICAPP '06), Reno, NV, USA, June 4-8, (2006).
16. M. Lindeburg, *Mechanical Engineering Reference Manual*, 11th Ed. Professional Publications, Inc., Belmont, California, (2001).
17. F.J. Moody, *Introduction to Unsteady Thermofluid Mechanics*, J. Wiley & Sons, New York, NY, (1990).
18. B. Munson, D. Young and T. Okiishi, *Fundamentals of Fluid Mechanics*, John Wiley & Sons, New York, 3rd Ed, (1998).
19. R. Newman and J. Payne, "The Burning Rates of Sodium Pool Fires," Combustion and Flame, Vol. 33, pp. 291-297, (1978).
20. Z. Renjun, J. Xinzhen, L. Baozhang, Z. Yong, and Z. Laiqi, "Studies on Gas Holdup in a Bubble Column Operated at Elevated Temperatures," Ind. Eng. Chem. Res, Vol. 27, pp. 1910-1916, (1988).
21. R. Span, and W. Wagner, "A New Equation of State for Carbon Dioxide Covering the Fluid Region from the Triple-Point Temperature to 1100K at Pressure up to 800 MPa", J. Phys. Chem Ref. Data, Vol. 25(6), pp. 1509-1596, (1996).
22. N.E. Todreas, and M.S. Kazimi, *Nuclear Systems I: Thermal Hydraulic Fundamentals*, Taylor & Francis, (1990).
23. G.B. Wallis, *One-Dimensional Two-Phase Flow*, McGraw-Hill, New York, NY, (1969).
24. N. Zuber and J. A. Findlay, "Average Volumetric Concentration in Two-Phase Flow Systems," J. Heat Transfer, Vol. 87, pp. 453–468, (1965).

Nuclear Engineering Division
Argonne National Laboratory
9700 South Cass Avenue
Argonne, IL 60439

www.anl.gov

Argonne National Laboratory is a U.S. Department of Energy
laboratory managed by UChicago Argonne, LLC